[AMERICAN JOURNAL OF SCIENCE, VOL. 310, NOVEMBER, 2010, P. 951-980, DOI 10.2475/09.2010.08]

# CA. 850 MA BIMODAL VOLCANIC ROCKS IN NORTHEASTERN JIANGXI PROVINCE, SOUTH CHINA: INITIAL EXTENSION DURING THE BREAKUP OF RODINIA?

W. X. LI*,**,†, X. H. LI***, and Z. X. LI** Fn*

**ABSTRACT. Multiple Meso- to Neoproterozoic magmatic events in South China are believed to record the transition in tectonic regime from the assembly of the supercontinent Rodinia to its breakup. We document in this paper the earliest, ca. 850 Ma bimodal volcanism in South China which may indicate the beginning of continental extension and rifting. The Zhenzhushan bimodal volcanic rocks were dated at 849 ± 6 Ma using the secondary ion mass spectrometry (SIMS) U-Pb zircon method. The mafic members of the succession are Si-saturated tholeiitic basalts with moderate enrichment in most incompatible trace elements and high εNd(T) values of 2.1 to 4.8. This suggests a likely derivation of the basalts from a depleted asthenospheric mantle source in an extensional environment, and that the magma experienced low-degree fractional crystallization and crustal contamination during its ascent to the surface. The felsic members are peraluminous and are characterized by negative εNd(T) values of −0.3 to −1.9 with geochemical features similar to those of the adjacent ca. 820 Ma peraluminous granitoids derived from a Mesoproterozoic to earliest Neoproterozoic sedimentary source. In combination with the distribution of 850 to 830 Ma igneous and sedimentary successions in South China, we suggest that continental rifting along the southern margin of the Yangtze Block probably started by 850 Ma. Coeval anorogenic magmatism has also been reported in other parts of the Rodinia supercontinent, and may represent the early stage of the Rodinia superplume in response to a circum-Rodinia mantle avalanche after the complete assembly of the supercontinent.**

Key words: Neoproterozoic, Rift magmatism, Yangtze Block, South China, Rodinia supercontinent, Superplume.

## INTRODUCTION

It is widely believed that the supercontinent Rodinia existed during the early Neoproterozoic (Hoffman, 1991; Moores, 1991; Dalziel, 1991; Z. X. Li and others, 2008). In central and eastern South China, orogenic-related magmatism ceased by ~890 Ma (Ye and others, 2007; Z. X. Li and others, 2007; W. X. Li and others, 2008a; X. H. Li and others 2009a), followed by a burst of intraplate magmatism between ca. 825 Ma and 750 Ma, with the latter being interpreted as the result of mantle plumes or a superplume after the amalgamation of the supercontinent Rodinia (Z. X. Li and others, 1999, 2003, 2008; X. H. Li and others, 2002, 2003a, 2008; W. X. Li and others, 2005, 2008b; Lin and others, 2007; X. C. Wang and others, 2007, 2008, 2009). There appears to be a magmatic quiescence between ca. 880 Ma and 825 Ma, apart from a small number of intrusive rocks (X. H. Li, 2008, 2010). Ca. 825 Ma has thus been regarded as the starting time of continental rifting in South China and elsewhere that eventually led to the break-up of Rodinia (Z. X. Li and others, 1999; X. H. Li and others, 2003a, 2008; W. X. Li and others, 2008b).

A suite of low-grade metasedimentary rocks crop-out along the southeastern margin of the Yangtze Block (fig. 1A), and were traditionally assigned to the Mesopro- F1

* Key Laboratory of Isotope Geochronology and Geochemistry, Guangzhou Institute of Geochemistry, Chinese Academy of Sciences, 511 Kehua Street, Guangzhou 510640, China
** The Institute for Geoscience Research, Department of Applied Geology, Curtin University of Technology, GPO Box U1987, Perth, WA 6845, Australia
*** State Key Laboratory of Lithospheric Evolution, Institute of Geology and Geophysics, Chinese Academy of Sciences, P.O. Box 9825, Beijing 100029, China
† Corresponding author: E-mail: liwx@gig.ac.cn; Fax: +86 20 85290130

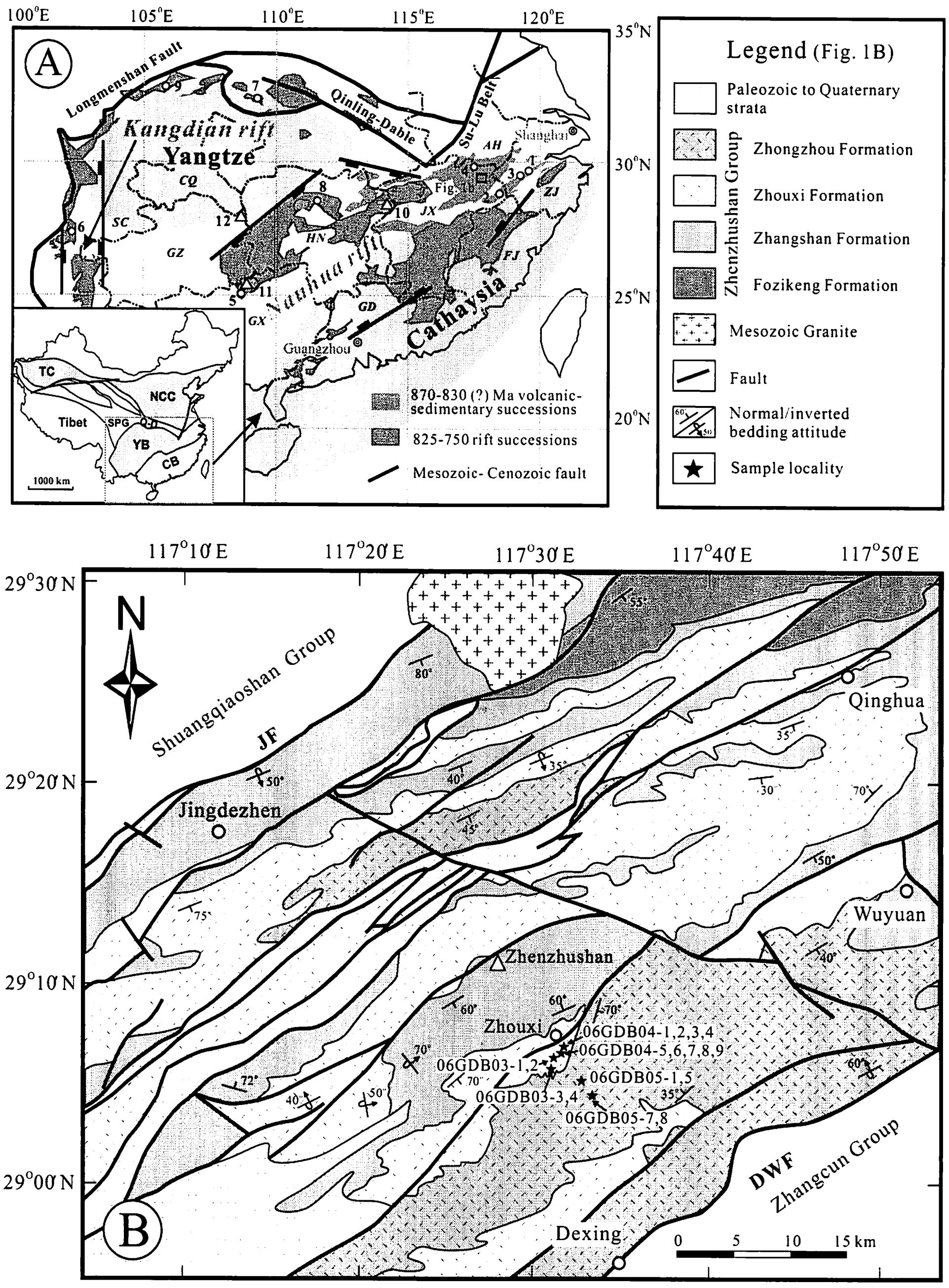


Fig. 1. (A) Distribution of mid-Neoproterozoic volcanic sedimentary rocks and rift basins in the South China Block. DWF: Dexing-Wuyuan Fault; JF: Jingdezhen Fault. Source of information: 1—838 ± 5 Ma Chencai bimodal volcanic rocks and 841 ± 6 Ma Lipu diorite (Z. X. Li and others, 2010); 2—848 ± 4 Ma Ganbian syenitic complex (X. H. Li and others, 2010); 3—849 ± 7 Ma Shenwu doleritic dyke (X. H. Li and others, 2008); 4—≤770 Ma Shuangqiaoshan quartz-keratophyres (X. L. Wang and others, 2008; X. H. Li and others, 2009a); 5—836 ± 3 Ma Zhaigun granodiorite (X. L. Wang and others, 2006); 6—857 ± 13 Ma Guandaoshan diorite (X. H. Li and others, 2003b; Sun and Zhou, 2008); 7—844 ± 2 Ma Fangcheng syenite (Bao and others, 2008); 8—823 ± 6 Ma Yiyang Komatiitic basalt (X. C. Wang and others, 2007); 9—820–810 Ma Bikou continental flood basalts (X. C. Wang and others, 2008); 10—ca. 860 Ma detritic zircons in the Lengjiaxi Formation (X. L. Wang and others, 2007); 11—860–870 Ma detritic zircons in the

terozoic, but they were recently reported to contain abundant 870 to 850 Ma detrital zircons (X. L. Wang and others, 2007, 2008; Zhou and others, 2009). These sequences are locally unconformably overlain by ~820 Ma rift-related volcanic-sedimentary rocks. Therefore, at least some of them should have formed within the ca. 880 to 820 Ma interval, a period considered by some to mark the transition in tectonic regime from a compressional environment to an extensional one (for example, X. H. Li and others, 2010). However, due to the lack of in-depth studies on these rocks, little is known regarding whether the formation of these rocks was related to the ≥880 Ma Sibao orogeny (Z. X. Li and others, 2002, 2007; W. X. Li and X. H. Li, 2003; X. H. Li and others, 2006, 2009a; Ye and others, 2007; W. X. Li and others, 2008a), or the younger rifting events, or neither. X. L. Wang and others (2007, 2008) regarded these sedimentary sequences as being formed in a back arc basin, thus implying post-880 Ma termination of the Sibao orogeny (the orogenic event representing the assembly of the Yangtze and Cathaysia blocks). On the other hand, geochemical studies of minor ~850 Ma syenites and dolerite dikes by X. H. Li and others (2008, 2010) suggest an intraplate setting, either due to orogenic collapse or an initial rifting event related to the break up of Rodinia.

Recent geological mapping in central-eastern South China (fig. 1A) identified some volcanic rocks in the post-880 Ma, but pre-820 Ma, successions (Deng and others, 2003). In this paper, we report a 849 ± 6 Ma secondary ion mass spectrometer (SIMS) U-Pb zircon age for one of the volcanic units, and geochemical and Nd isotopic data for the bimodal volcanic succession in northeastern Jiangxi Province (fig. 1A), Yangtze Block, South China. Our new data suggest that extension-related magmatism started at the southeastern margin of the Yangtze Block as early as ca. 850 Ma, which is about 50 Ma after the final amalgamation of the supercontinent Rodinia and 20 to 30 Ma before the first major breakout of plume-related magmatism. We speculate that coeval ca. 850 Ma extension-related magmatic events in other parts of Rodinia may indicate the early onset of the Rodinian superplume that eventually broke up the supercontinent.

## GEOLOGICAL BACKGROUND AND PETROGRAPHY

The South China Block is considered to have formed through the amalgamation of the Yangtze and Cathaysia blocks during the Late Mesoproterozoic to early Neoproterozoic Sibao orogeny (Cheng, 1991, 1993; Z. X. Li and others, 2002, 2007, 2008; Ye and others, 2007; X. H. Li and others, 2009a). Along the southeastern boundary of the Yangtze Block, there is a widespread suite of dominantly marine clastic sedimentary rocks (fig. 1A, shown as ca. 870-830 Ma volcanic-sedimentary successions). These strata have different names in different regions, that is, the traditional Shuangqiaoshan Group in Jiangxi, the Lengjiaxi Group in Hunan, the Sibao Group in northern Guangxi and the Fangjingshan Group in northern Guizhou (fig. 1A). Due to the lack of reliable isotopic ages, these strata were previously considered as Mesoproterozoic sedimentary units, but recent work shows that <880 Ma detrital zircons are abundant in these rocks, suggesting Neoproterozoic rather than Mesoproterozoic ages for these rocks (X. L. Wang and others, 2007; Zhou and others, 2009). These strata are locally unconformably overlain by Neoproterozoic (<825 Ma), volcanic-sedimentary rift

Sibao Group (X. L. Wang and others, 2007); 12—869–874 Ma detritic zircons in the Fanjingshan Group (Zhou and others, 2009). ZJ—Zhejiang Province; AH—Anhui Province; JX—Jiangxi Province; HN—Hunan Province; GX—Guangxi Province; FJ—Fujiang Province; GD—Guangdong Province; CQ—Chongqing city; SC—Sichuan Province. The insert shows the main tectonic units in China and the location of South China Block. TC—Tarim Craton; NCC—North China Craton; YB—Yangtze Block; CB—Cathaysia Block; SPG—Songpan-Ganzi Belt; Q-D—Qinling-Dabie Belt. (B) Geological map showing the distribution of the Zhenzhushan Group volcanic-sedimentary rocks in northeastern Jiangxi Province, South China (modified after the 1:25000 geological map), and the sampling localities.

successions (called the Dengshan Group in northeastern Jiangxi Province) and have undergone strong deformation and lower greenschist-facies metamorphism, possibly during the Early Paleozoic (Wuyi-Yunkai, or "Caledonian") and/or during the Mesozoic Indonesian tectonic event (Z. X. Li and others, 2010).

Recent geological mapping in northeastern Jiangxi Province subdivided the Shuangqiaoshan Group into three lithologic units, that is, the Zhangcun Group, the Zhenzhushan Group and the Shuangqiaoshan Group (Deng and others, 2003), separated by faults (fig. 1B). The Zhenzhushan Group contains mafic and felsic volcanic rocks as well as volcaniclastic sedimentary rocks (Deng and others, 2003). It crops out between the Dexing-Wuyuan Fault and the Jingdezhen Fault, and has been subdivided into four formations, from the bottom to the top: the Fozikeng, Zhangshan, Zhouxi and Zhongcun formations (figs. 1B and 2). The Fozikeng and Zhangshan formations consist mainly of argillaceous phyllite and graywacke sandstones with turbititic structures, with total thicknesses of ca. 1450 and 1460 m, respectively. The Zhouxi and Zhongcun formations comprise dominantly felsic pyroclastic rocks interlayered with basalts and dacite, with thicknesses of ca. 1120 and 1130 m, respectively (fig. 2). The basaltic layers occur dominantly in the upper part of the Zhouxi Formation with thicknesses of between several meters to tens of meters. The felsic rocks are dominantly volcaniclastic, with minor dacite. The Zhenzhushan Group is locally unconformably overlain by Neoproterozoic volcanic-sedimentary strata called the Dengshan Group. It is noted that the thickness of the Zhenzhushan Group was possibly over-estimated due to structural duplication of the unit. F2

The mafic volcanic rocks of the Zhouxi Formation are dominantly altered basalts with loss on ignition (LOI) of 7.08 to 18.43 weight percent. The basalts are dark-green in color, consisting of 30 to 40 percent plagioclase, 3 to 5 percent quartz, and 40 to 55 percent mafic minerals that have been extensively altered/metamorphosed to chlorite and biotite. Rare relict pyroxene has been observed. The dacites are light-gray in color, containing abundant (30-40%) plagioclase, 30 to 50 percent quartz and 20 to 30 percent biotite as well as minor Fe-Ti oxides and 1 to 5 percent plagioclase and quartz phenocrysts. All rocks underwent strong deformation and greenschist facies metamorphism.

## ANALYTICAL METHODS

Zircons were separated using standard density and magnetic techniques. Zircon grains, together with zircon U-Pb standard TEMORA, were cast in an epoxy mount, which was then ground and polished to section the crystals in half for analysis. Zircons were imaged in transmitted and reflected light and by cathodoluminescence (CL) as a guide for analytical spot selection. U-Pb isotopic compositions were analyzed using the Cameca IMS 1280 ion microprobe at the Institute of Geology and Geophysics, Chinese Academy of Sciences. U-Th-Pb ratios were determined relative to the TEMORA standard zircon with $^{206}Pb/^{238}U = 0.0668$ corresponding to 417 Ma (Black and others, 2003), and the absolute abundances were calibrated to the standard zircon M257 (Nasdala and others, 2008). Analyses of the TEMORA standard zircon were interspersed with those of the unknown grains, following operating and data processing procedures similar to those described by X. H. Li and others (2009b). The mass resolution used to measure Pb/Pb and Pb/U isotopic ratios was 5400 during the analyses. The uncertainty of 1.5 percent (1 RSD) for $^{206}Pb/^{238}U$ measurements of the standard zircons was propagated to the unknowns (Q. L. Li and others, 2010), despite that the measured $^{206}Pb/^{238}U$ error in a specific session is generally around 1 percent (1 RSD) or less. Compositions were corrected for common Pb using measured non-radiogenic $^{204}Pb$. Corrections are sufficiently small to be insensitive to the choice of common Pb composition, and an average of present-day crustal composition (Stacey and Kramers, 1975) was used for the common Pb correction assuming that the

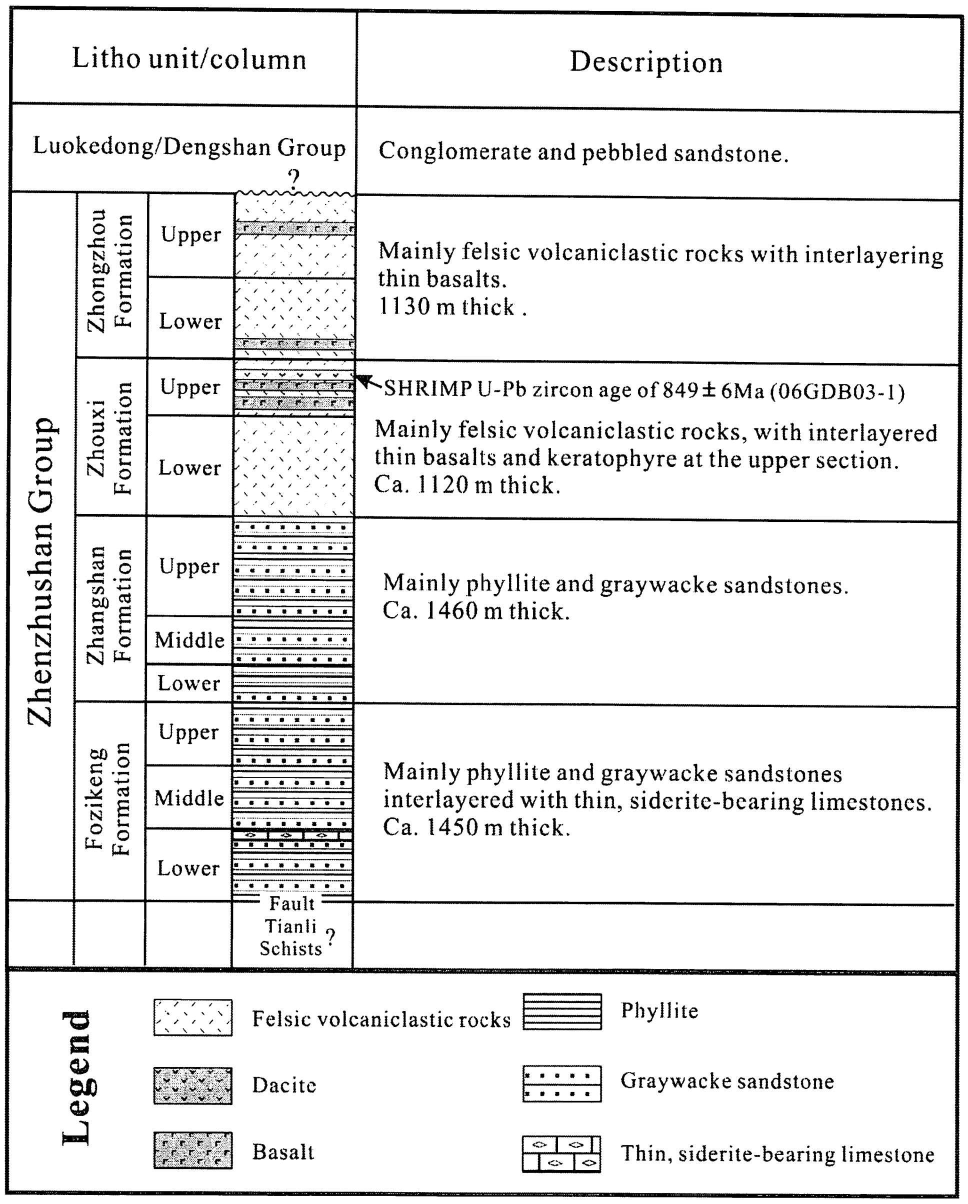


Fig. 2. Stratigraphic column of the Zhenzhushan Group in northeastern Jiangxi, South China (after Deng and others, 2003).

common Pb is largely surface contamination introduced during sample preparation. Uncertainties on individual analyses are reported at the 1$\sigma$ level, and mean ages for pooled $^{206}Pb/^{238}U$ results are quoted at the 95 percent confidence level. Data reduction was carried out using the Isoplot/Ex v. 2.49 program (Ludwig, 2001).

Major element oxides and trace elements were determined using a Rigaku ZSK100e XRF on fused glass beads and a Perkin-Elmer Sciex ELAN 6000 ICP-MS, respectively, at the Guangzhou Institute of Geochemistry, Chinese Academy of Sciences. Analytical procedures were similar to those described by X. H. Li and others (2000, 2005). A mixture of 0.5 g powdered sample and 4 g $Li_2B_4O_7$ was fused as a glass bead for XRF analysis. Loss-on-ignition (LOI) measurements were undertaken on samples of dried rock powder by heating in a pre-ignition silica crucible to 1000°C for one hour and recording the percentage weight loss. Analytical uncertainties of major elements are between 1 percent and 5 percent. About 50 milligrams of each powdered sample were dissolved in a high-pressure Teflon bomb for 24 hrs using a $HF+HNO_3$ mixture to ensure complete sample digestion. Rh was used as an internal standard to monitor signal drift during analysis. The USGS standards BCR-1, BHVO-1, W-2, G-2, and GSP-1 were used for calibrating element concentrations of measured samples. Analytical precision is generally better than 3 percent for most trace elements.

The Nd fraction was separated by passing through cation columns followed by HDEHP columns. Nd isotopic compositions were determined using a Micromass Isoprobe multi-collector ICP-MS (MC-ICP-MS) at the Guangzhou Institute of Geochemistry. Analytical procedures were similar to those described by X. H. Li and others (2004). Samples were taken up in 2 percent $HNO_3$, and the aqueous solutions were introduced into the MC-ICPMS using a Meinhard glass nebulizer with an uptake rate of 0.1 ml/minute. The inlet system was washed out for five minutes between analyses using high-purity 5 percent $HNO_3$ followed by a blank solution of 2 percent $HNO_3$ from which the sample solutions were prepared. The Isoprobe MC-ICPMS was operated in a static mode, and yielded $^{143}Nd/^{144}Nd = 0.512125 \pm 11$ ($2\sigma$) on 14 runs for the Shin Etsu JNdi-1 standard during this study. Measured $^{143}Nd/^{144}Nd$ ratios were normalized to $^{146}Nd/^{144}Nd = 0.7219$. The reported $^{143}Nd/^{144}Nd$ ratios are adjusted relative to the Shin Etsu JNdi-1 standard of 0.512115, corresponding to the La Jolla standard of 0.511860 (Tanaka and others, 2000).

## RESULTS

### *U-Pb Zircon Age*

Dacite sample 06GDB03-1 (29°06′31″N; 117°31′40″E) was collected from the upper part of the Zhouxi Formation near the Zhouxi village (fig. 1B). Zircon grains from this sample are mostly euhedral, 50 to 150 μm long with length to width ratios of 1:1 to 2:1. They are transparent and colorless. Oscillatory zoning is common in most zircons in CL images (fig. 3 inset), with a few grains showing cores. Sixteen analyses were conducted on 16 zircon grains in sets of 7 scans during a single session (table 1). The analyses gave variable abundances of U (59-313 ppm) and Th (35-242 ppm) with Th/U ratios mostly in the range of between 0.5 and 0.9, comparable to typical magmatic zircon. The common Pb content is low with $f_{206} < 0.25$ percent. Fourteen of 16 analyses (excluding spots 7 and 12) gave concordant results within analytical errors, and the weighted mean of $^{207}Pb/^{206}Pb$, $^{207}Pb/^{235}U$ and $^{206}Pb/^{238}U$ ages are 845 ± 10 Ma, 848 ± 6 Ma and 851 ± 6 Ma, respectively. The calculated Concordia age of 849 ± 6 Ma (95% confidence interval) is considered the best estimate of the crystallization age of the dacite (fig. 3). Spots 7 and 12 yielded older $^{206}Pb/^{238}U$ and $^{207}Pb/^{206}Pb$ ages of ca. 920 and ca. 1000 Ma, respectively (table 1 and fig. 3). They are likely to be xenocrysts, similar in age to the ca. 1.0 to 0.9 Ga igneous rocks from the Shuangxiwu magmatic arc (Ye and others, 2007; X. H. Li and others, 2009a).

F3 T1

### *Major and Trace Element Geochemistry*

Seventeen samples of the Zhenzhushan volcanic rocks were analyzed for their major and trace element concentrations. The results are listed in table 2. T2c

Considering that the Zhenzhushan volcanic rocks have undergone strong alteration with high values of loss on ignition (LOI) of 1.79 to 6.20 weight percent for felsic rocks and 7.08 to 18.43 weight percent for mafic rocks, the contents of mobile

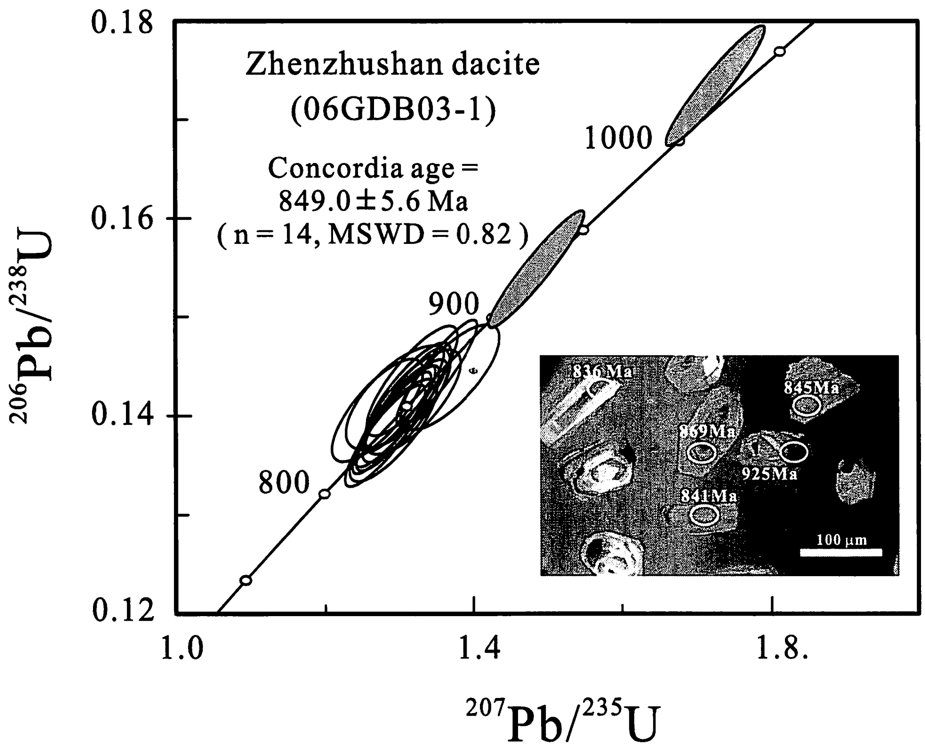


Fig. 3. U-Pb concordia diagram showing the analytical data for zircons from dacite sample 06GDB03-1 from the Zhenzhushan Group. The gray ellipses represent xenocrysts and were excluded from the calculation of the concordia age.

components might have been modified (Romer and others, 2001). Therefore, the effect of alteration and the mobility of the major and trace elements were evaluated prior to geochemical characterizations and petrological discussions of the studied rocks.

The CIA value [$Al_2O_3$/($Al_2O_3$+CaO+$Na_2O$+$K_2O$) in molecular proportions] of a rock has been regarded an important index for evaluating its alteration and chemical weathering effects (Nesbitt and Young, 1982; Young, 2009). The CIA values of the studied mafic rocks are in a range of 40 to 61, with the least-altered sample overlapping that of fresh basalts (CIA = 30-45, Nesbitt and Young, 1982). The felsic rocks have CIA values of 54 to 67, slightly above those for fresh granitic rocks (CIA = 45-55, Nesbitt and Young, 1982). On the A-CN-K triangular diagram of Nesbitt and Young (1989), the mafic rocks define a trend paralleling the A-CN boundary toward the "A" apex (fig. 4A), indicating formation of clay minerals during alteration. The felsic rocks trend towards the A-K boundary, suggesting K-metasomatism forming muscovite and/or sericite as observed in thin sections. On the A-CNK-FM triangular diagram of Nesbitt and Young (1989), the mafic rocks trend toward the A-FM boundary (fig. 4B), indicating alteration of some ferromagnesian-bearing minerals. In the $FeO^t$ vs. MgO and CaO vs. $Al_2O_3$ diagrams (figs. 4C and 4D), the mafic rocks plot toward chlorite, suggesting chloritization as the dominant alteration for the mafic components. This is compatible with the petrographic observations. F4

In order to evaluate the mobility of elements, some major and trace elements are plotted against the CIA value (fig. 5). The high field-strength elements (HFSE: Zr, Nb, F5

TABLE 1

*SIMS U-Pb zircon data*

| Sample spot # | U ppm | Th ppm | Th/U | $f_{206}$ (%) | $^{207}Pb/^{206}Pb$ | ±1s (%) | $^{207}Pb/^{235}U$ | ±1σ (%) | $^{206}Pb/^{238}U$ | ±1σ (%) | Age 207/206 (Ma) | ±1σ | Age 207/235 (Ma) | ±1σ | Age 206/238 (Ma) | ±1σ |
|---|---|---|---|---|---|---|---|---|---|---|---|---|---|---|---|---|
| 06DGB03-1-1 | 82 | 53 | 0.61 | 0.07 | 0.0676 | 1.31 | 1.318 | 2.00 | 0.1414 | 1.51 | 857 | 27 | 854 | 12 | 853 | 12 |
| 06DGB03-1-2 | 267 | 242 | 0.85 | 0.06 | 0.0669 | 0.73 | 1.307 | 1.67 | 0.1416 | 1.50 | 836 | 15 | 849 | 10 | 854 | 12 |
| 06DGB03-1-3 | 149 | 143 | 0.89 | 0.00 | 0.0676 | 1.09 | 1.292 | 1.87 | 0.1386 | 1.52 | 857 | 23 | 842 | 11 | 836 | 12 |
| 06DGB03-1-4 | 59 | 35 | 0.56 | 0.14 | 0.0664 | 1.63 | 1.298 | 2.22 | 0.1418 | 1.51 | 818 | 34 | 845 | 13 | 855 | 12 |
| 06DGB03-1-5 | 243 | 201 | 0.78 | 0.02 | 0.0679 | 0.71 | 1.351 | 1.66 | 0.1444 | 1.50 | 864 | 15 | 868 | 10 | 869 | 12 |
| 06DGB03-1-6 | 183 | 129 | 0.66 | 0.02 | 0.0673 | 0.85 | 1.281 | 1.73 | 0.1380 | 1.51 | 847 | 17 | 837 | 10 | 833 | 12 |
| 06DGB03-1-7 | 305 | 223 | 0.69 | 0.03 | 0.0696 | 0.64 | 1.487 | 1.63 | 0.1550 | 1.50 | 916 | 13 | 925 | 10 | 929 | 13 |
| 06DGB03-1-8 | 190 | 202 | 1.00 | 0.05 | 0.0670 | 0.84 | 1.294 | 1.72 | 0.1400 | 1.50 | 839 | 17 | 843 | 10 | 845 | 12 |
| 06DGB03-1-9 | 68 | 35 | 0.47 | 0.05 | 0.0690 | 1.33 | 1.369 | 2.00 | 0.1439 | 1.50 | 898 | 27 | 876 | 12 | 867 | 12 |
| 06DGB03-1-10 | 108 | 100 | 0.86 | 0.03 | 0.0666 | 1.08 | 1.317 | 1.91 | 0.1435 | 1.58 | 824 | 22 | 853 | 11 | 865 | 13 |
| 06DGB03-1-11 | 90 | 67 | 0.69 | 0.25 | 0.0655 | 1.29 | 1.270 | 1.98 | 0.1406 | 1.50 | 792 | 27 | 833 | 11 | 848 | 12 |
| 06DGB03-1-12 | 313 | 131 | 0.39 | 0.00 | 0.0722 | 0.56 | 1.725 | 1.60 | 0.1734 | 1.50 | 990 | 11 | 1018 | 10 | 1031 | 14 |
| 06DGB03-1-13 | 139 | 80 | 0.54 | 0.03 | 0.0669 | 1.02 | 1.311 | 1.82 | 0.1421 | 1.51 | 835 | 21 | 851 | 11 | 856 | 12 |
| 06DGB03-1-14 | 206 | 166 | 0.75 | 0.00 | 0.0673 | 0.85 | 1.298 | 1.77 | 0.1398 | 1.55 | 848 | 18 | 845 | 10 | 843 | 12 |
| 06DGB03-1-15 | 129 | 74 | 0.54 | 0.02 | 0.0675 | 1.01 | 1.307 | 1.81 | 0.1405 | 1.50 | 853 | 21 | 849 | 10 | 848 | 12 |
| 06DGB03-1-16 | 232 | 226 | 0.91 | 0.04 | 0.0671 | 0.77 | 1.290 | 1.69 | 0.1393 | 1.50 | 842 | 16 | 841 | 10 | 841 | 12 |
| **Average (outliers 7 & 12)** | | | | | | | | | | | **845** | **10** | **848** | **6** | **851** | **6** |

$f_{206}$ is the percentage of common $^{206}Pb$ in total $^{206}Pb$.

TABLE 2

*Major and trace element data for the Zhenzhushan volcanic rocks*

| | 06GDB3-1 | 06GDB3-2 | 06GDB3-3 | 06GDB3-4 | 06GDB4-9 | 06GDB5-1 | 06GDB5-5 |
|---|---|---|---|---|---|---|---|
| Location | 29°06'31"N; 117°31'40"E | 29°06'31"N; 117°31'40"E | 29°05'25"N; 117°31'22"E | 29°05'25"N; 117°31'22"E | 29°06'40"N; 117°31'51"E | 29°05'23"N; 117°32'49"E | 29°05'23"N; 117°32'49"E |
| Rock name | dacite | dacite | dacite | dacite | dacite | dacite | dacite |
| Major oxides (%) | | | | | | | |
| $SiO_2$ | 71.94 | 73.60 | 71.79 | 67.60 | 72.81 | 70.60 | 73.73 |
| $TiO_2$ | 0.74 | 0.70 | 0.67 | 0.84 | 0.67 | 0.79 | 0.74 |
| $Al_2O_3$ | 14.34 | 13.02 | 13.34 | 16.56 | 13.18 | 14.82 | 12.11 |
| $Fe_2O_3$ | 5.23 | 5.40 | 6.08 | 6.81 | 6.25 | 5.60 | 5.84 |
| MnO | 0.07 | 0.10 | 0.10 | 0.11 | 0.10 | 0.08 | 0.11 |
| MgO | 1.41 | 1.39 | 1.73 | 1.92 | 1.59 | 1.48 | 1.44 |
| CaO | 0.80 | 0.61 | 0.85 | 0.60 | 0.36 | 0.55 | 0.95 |
| $Na_2O$ | 3.80 | 2.38 | 3.77 | 1.91 | 2.90 | 2.51 | 2.30 |
| $K_2O$ | 2.17 | 2.21 | 1.60 | 3.54 | 2.20 | 3.07 | 2.11 |
| $P_2O_5$ | 0.14 | 0.13 | 0.12 | 0.15 | 0.13 | 0.14 | 0.14 |
| Total | 100.65 | 99.55 | 100.05 | 100.04 | 100.21 | 99.63 | 99.47 |
| LOI | 4.51 | 4.57 | 5.07 | 6.20 | 4.26 | 2.24 | 2.28 |
| Mg# | | | | | | | |
| ACNK | 1.43 | 1.76 | 1.41 | 2.05 | 1.69 | 1.75 | 1.55 |
| Q | 37. 9 | 48. 5 | 39.7 | 39.2 | 44.6 | 41.4 | 48.8 |
| CIA | 0.59 | 0.64 | 0.58 | 0.67 | 0.63 | 0.64 | 0.61 |
| Trace elements (ppm) | | | | | | | |
| Sc | 11.5 | 10.8 | 11.3 | 14.5 | 11.0 | 13.6 | 11.1 |
| V | 82.0 | 70.6 | 73.4 | 94.5 | 71.4 | 92.6 | 65.8 |
| Cr | 52.5 | 49.2 | 47.5 | 51.2 | 51.1 | 68.2 | 79.8 |
| Co | 10.5 | 11.5 | 14.9 | 16.2 | 14.9 | 13.6 | 12.6 |
| Ni | 20.3 | 21.3 | 24.5 | 29.4 | 25.3 | 27.1 | 25.3 |
| Ga | 16.2 | 14.8 | 15.7 | 19.8 | 15.1 | 18.9 | 14.4 |
| Rb | 93.5 | 92.1 | 68.5 | 147 | 91.6 | 137 | 88.1 |
| Sr | 142 | 115 | 156 | 105 | 100 | 111 | 105 |
| Y | 28.3 | 23.5 | 27.4 | 29.8 | 24.7 | 30.4 | 28.8 |
| Zr | 225 | 230 | 206 | 207 | 224 | 236 | 282 |
| Nb | 11.5 | 11.0 | 10.6 | 12.6 | 10.7 | 13.8 | 10.1 |
| Ba | 351 | 318 | 271 | 428 | 280 | 410 | 219 |
| La | 32.4 | 35.1 | 30.7 | 34.7 | 33.7 | 35.3 | 34.0 |
| Ce | 64.6 | 71.7 | 63.6 | 73.6 | 70.4 | 73.9 | 69.6 |
| Pr | 7.42 | 8.26 | 7.27 | 8.62 | 7.99 | 8.56 | 8.90 |
| Nd | 29.6 | 32.8 | 29.4 | 34.7 | 31.8 | 34.7 | 33.8 |
| Sm | 5.52 | 6.05 | 5.83 | 6.80 | 6.00 | 6.53 | 6.333 |
| Eu | 1.21 | 1.38 | 1.32 | 1.40 | 1.34 | 1.35 | 1.31 |
| Gd | 5.32 | 5.48 | 5.50 | 6.40 | 5.65 | 6.15 | 5.42 |
| Tb | 0.87 | 0.83 | 0.87 | 1.01 | 0.87 | 0.99 | 0.86 |
| Dy | 5.17 | 4.63 | 5.04 | 5.86 | 4.92 | 5.71 | 4.92 |
| Ho | 1.04 | 0.89 | 1.00 | 1.16 | 0.96 | 1.16 | 1.01 |
| Er | 3.05 | 2.64 | 2.90 | 3.46 | 2.74 | 3.35 | 2.78 |
| Tm | 0.46 | 0.40 | 0.44 | 0.53 | 0.42 | 0.52 | 0.40 |
| Yb | 3.01 | 2.65 | 2.97 | 3.45 | 2.80 | 3.48 | 2.76 |
| Lu | 0.48 | 0.41 | 0.45 | 0.54 | 0.43 | 0.53 | 0.41 |
| Hf | 6.03 | 6.10 | 5.55 | 6.12 | 6.16 | 6.87 | 6.88 |
| Ta | 0.83 | 0.76 | 0.78 | 0.99 | 0.79 | 1.14 | 0.78 |
| Pb | 8.50 | 18.0 | 12.2 | 27.7 | 16.7 | 6.64 | 12.7 |
| Th | 10.3 | 10.2 | 10.2 | 12.8 | 10.6 | 16.0 | 11.0 |
| U | 2.35 | 2.07 | 1.90 | 2.75 | 2.40 | 3.67 | 2.24 |

TABLE 2

*(continued)*

| | 06GDB5-7 | 06GDB5-8 | 06GDB4-1 | 06GDB4-2 | 06GDB4-3 | 06GDB4-4 | 06GDB4-5 |
|---|---|---|---|---|---|---|---|
| Location | 29°04'21"N; 117°33'21"E | 29°04'21"N; 117°33'21"E | 29°06'55"N; 117°31'58"E | 29°06'55"N; 117°31'58"E | 29°06'55"N; 117°31'58"E | 29°06'55"N; 117°31'58"E | 29°06'40"N; 117°31'51"E |
| Rock name | dacite | dacite | basalt | basalt | basalt | basalt | basalt |
| Major oxides (%) | | | | | | | |
| $SiO_2$ | 73.32 | 71.24 | 52.06 | 51.61 | 52.17 | 49.84 | 49.64 |
| $TiO_2$ | 0.46 | 0.73 | 1.41 | 1.40 | 1.39 | 1.13 | 1.13 |
| $Al_2O_3$ | 14.52 | 14.48 | 17.75 | 17.74 | 17.55 | 17.00 | 16.71 |
| $Fe_2O_3$ | 2.94 | 5.72 | 13.06 | 12.89 | 13.29 | 12.70 | 12.63 |
| MnO | 0.06 | 0.07 | 0.16 | 0.15 | 0.15 | 0.17 | 0.17 |
| MgO | 0.79 | 1.44 | 7.89 | 7.98 | 8.04 | 10.15 | 10.26 |
| CaO | 1.12 | 0.37 | 4.20 | 5.03 | 3.89 | 6.58 | 7.17 |
| $Na_2O$ | 4.94 | 2.99 | 2.59 | 2.67 | 2.27 | 2.20 | 2.06 |
| $K_2O$ | 1.86 | 2.81 | 0.55 | 0.54 | 0.58 | 0.49 | 0.47 |
| $P_2O_5$ | 0.12 | 0.14 | 0.11 | 0.11 | 0.10 | 0.10 | 0.10 |
| Total | 100.12 | 99.98 | 99.79 | 100.12 | 99.42 | 100.34 | 100.34 |
| LOI | 1.79 | 1.93 | 11.93 | 12.66 | 11.41 | 12.64 | 7.08 |
| Mg# | | | 54.67 | 55.25 | 54.70 | 61.47 | 61.86 |
| ACNK | 1.19 | 1.68 | | | | | |
| Q | 34.2 | 40. 6 | 14.5 | 11.6 | 16.8 | 6.2 | 5.4 |
| CIA | 0.54 | 0.63 | 0.59 | 0.56 | 0.61 | 0.51 | 0.50 |
| Trace elements (ppm) | | | | | | | |
| Sc | 6.2 | 12.3 | 35.2 | 34.1 | 36.3 | 23.8 | 30.7 |
| V | 27.9 | 73.9 | 214 | 216 | 233 | 155 | 204 |
| Cr | 21.2 | 41.9 | 302 | 303 | 287 | 219 | 290 |
| Co | 3.73 | 11.9 | 47.2 | 45.9 | 46.3 | 35.2 | 48.1 |
| Ni | 8.96 | 22.4 | 157 | 150 | 152 | 109 | 140 |
| Ga | 15.5 | 17.1 | 19.0 | 18.5 | 18.6 | 12.5 | 15.7 |
| Rb | 86.3 | 127 | 21.5 | 20.6 | 23.8 | 14.5 | 21.0 |
| Sr | 307 | 133 | 100 | 112 | 95.2 | 68.8 | 90.4 |
| Y | 31.6 | 27.7 | 22.1 | 21.3 | 19.3 | 13.6 | 16.9 |
| Zr | 277 | 240 | 87 | 82.6 | 75.0 | 61.5 | 76.5 |
| Nb | 14.5 | 11.7 | 8.69 | 8.27 | 7.46 | 6.05 | 7.14 |
| Ba | 372 | 493 | 49.4 | 45.6 | 43.3 | 22.1 | 26.2 |
| La | 49.5 | 36.5 | 8.84 | 8.68 | 8.97 | 5.52 | 7.04 |
| Ce | 100 | 74.9 | 18.2 | 18.1 | 18.7 | 11.7 | 15.1 |
| Pr | 11.0 | 8.65 | 2.23 | 2.18 | 2.28 | 1.47 | 1.91 |
| Nd | 41.2 | 34.2 | 10.1 | 10.0 | 10.5 | 6.92 | 9.14 |
| Sm | 7.09 | 6.14 | 2.58 | 2.54 | 2.53 | 1.81 | 2.34 |
| Eu | 1.14 | 1.33 | 0.99 | 0.93 | 0.92 | 0.72 | 0.93 |
| Gd | 6.58 | 5.88 | 3.27 | 3.09 | 2.92 | 2.13 | 2.72 |
| Tb | 0.97 | 0.91 | 0.64 | 0.62 | 0.57 | 0.42 | 0.53 |
| Dy | 5.64 | 5.27 | 4.07 | 3.86 | 3.60 | 2.57 | 3.26 |
| Ho | 1.11 | 1.07 | 0.85 | 0.80 | 0.73 | 0.52 | 0.66 |
| Er | 3.37 | 3.17 | 2.33 | 2.19 | 1.99 | 1.34 | 1.82 |
| Tm | 0.51 | 0.47 | 0.34 | 0.33 | 0.31 | 0.21 | 0.27 |
| Yb | 3.44 | 3.16 | 2.21 | 2.12 | 1.91 | 1.33 | 1.74 |
| Lu | 0.51 | 0.49 | 0.34 | 0.33 | 0.29 | 0.21 | 0.27 |
| Hf | 8.39 | 6.80 | 2.09 | 1.89 | 1.77 | 1.17 | 1.66 |
| Ta | 1.41 | 0.85 | 0.53 | 0.49 | 0.43 | 0.29 | 0.40 |
| Pb | 18.9 | 12.3 | 12.5 | 12.4 | 12.2 | 9.99 | 13.9 |
| Th | 23.9 | 12.1 | 2.60 | 2.42 | 2.48 | 1.26 | 1.58 |
| U | 4.95 | 2.68 | 0.45 | 0.39 | 0.38 | 0.12 | 0.22 |

TABLE 2

*(continued)*

| | 06GDB4-6 | 06GDB4-7 | 06GDB4-8 |
|---|---|---|---|
| Location | 29°06'40"N; 117°31'51"E | 29°06'40"N; 117°31'51"E | 29°06'40"N; 117°31'51"E |
| Rock name | basalt | basalt | basalt |
| Major oxides (%) | | | |
| $SiO_2$ | 49.22 | 49.11 | 50.28 |
| $TiO_2$ | 1.15 | 1.21 | 1.37 |
| $Al_2O_3$ | 16.23 | 15.52 | 15.27 |
| $Fe_2O_3$ | 12.80 | 12.38 | 11.70 |
| MnO | 0.17 | 0.18 | 0.17 |
| MgO | 10.20 | 10.02 | 8.21 |
| CaO | 7.66 | 9.45 | 9.62 |
| $Na_2O$ | 1.67 | 1.82 | 2.79 |
| $K_2O$ | 0.51 | 0.22 | 0.64 |
| $P_2O_5$ | 0.10 | 0.11 | 0.13 |
| Total | 99.72 | 100.01 | 100.18 |
| LOI | 13.74 | 15.43 | 18.43 |
| Mg# | 61.40 | 61.76 | 58.35 |
| ACNK | | | |
| Q | 6.7 | 5.5 | 3.3 |
| CIA | 0.48 | 0.43 | 0.40 |
| Trace elements (ppm) | | | |
| Sc | 32.9 | 28.9 | 26.1 |
| V | 216 | 200 | 192 |
| Cr | 256 | 285 | 247 |
| Co | 46.8 | 46.5 | 40.2 |
| Ni | 122 | 145 | 112 |
| Ga | 15.9 | 15.5 | 14.9 |
| Rb | 20.0 | 6.84 | 22.4 |
| Sr | 86.1 | 115.6 | 198 |
| Y | 17.3 | 18.6 | 17.4 |
| Zr | 78. 7 | 87.9 | 92.2 |
| Nb | 7.33 | 8.04 | 9.50 |
| Ba | 26.9 | 24.6 | 99.0 |
| La | 7.18 | 8.60 | 9.19 |
| Ce | 15.4 | 18.6 | 20.2 |
| Pr | 2.00 | 2.38 | 2.54 |
| Nd | 9.49 | 10.9 | 11.7 |
| Sm | 2.46 | 2.77 | 2.90 |
| Eu | 0.96 | 0.97 | 0.88 |
| Gd | 2.84 | 3.06 | 3.07 |
| Tb | 0.55 | 0.59 | 0.57 |
| Dy | 3.37 | 3.61 | 3.40 |
| Ho | 0.68 | 0.71 | 0.66 |
| Er | 1.82 | 1.96 | 1.85 |
| Tm | 0.29 | 0.30 | 0.28 |
| Yb | 1.80 | 1.89 | 1.77 |
| Lu | 0.28 | 0.31 | 0.27 |
| Hf | 1.68 | 2.02 | 2.15 |
| Ta | 0.41 | 0.47 | 0.59 |
| Pb | 13.4 | 13.7 | 15.7 |
| Th | 1.57 | 2.68 | 2.91 |
| U | 0.21 | 0.42 | 0.51 |

Mg# = Mg/(Mg + $Fe_{2+}$), assuming $Fe_2O_3/(FeO + Fe_2O_3) = 0.20$. Total iron as $Fe_2O_3$. Q—Quartz content calculated by CIPW method; CIA—Alteration and weathering index ($Al_2O_3/Al_2O_3+CaO_2+Na_2O+K_2O$) in molecular proportion.

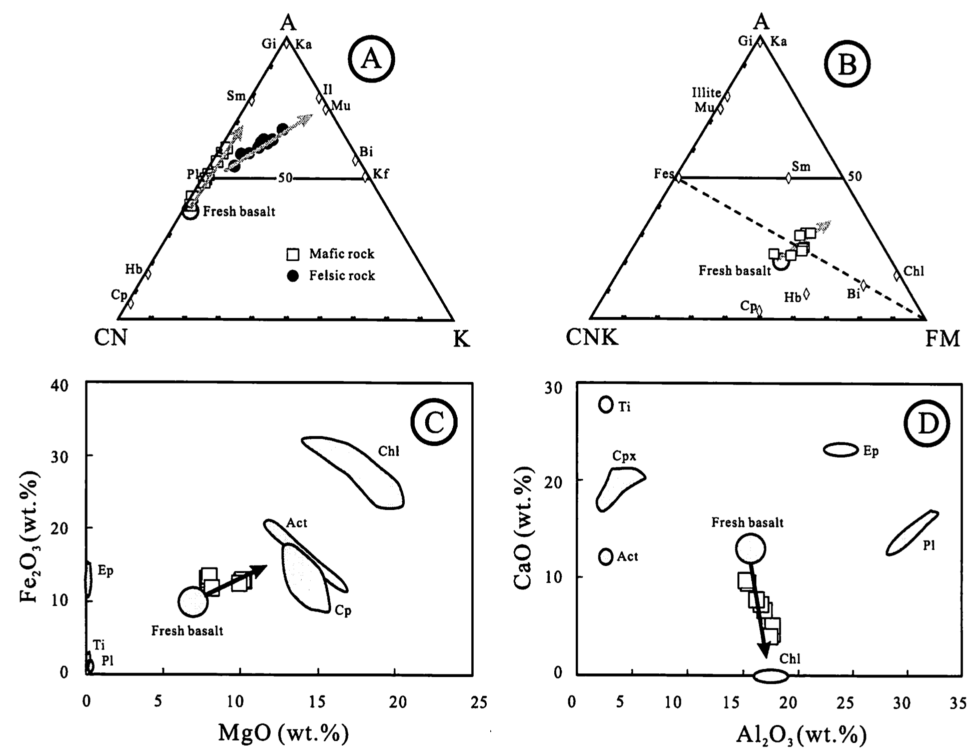


Fig. 4. (A) A-CN-K diagram (Nesbitt and Young, 1989) for evaluating the influence of alteration and weathering. (B) A-CNK-FM diagram (Nesbitt and Young, 1989) showing alteration of the ferromagnesian-bearing minerals in the mafic rocks. (C) $Fe_2O_3$ vs. MgO and (D) CaO vs. $Al_2O_3$ diagrams (after Teagle and Alt, 2004) showing probable chloritization of the mafic rocks. Abbreviations are: Act = actinolite; Bi = biotite; Chl = chlorite; Cp = clinopyroxene; Ep = epidote; Fes = plagioclase+K feldspar; Gi = gibbsite; Hb = hornblende; Il = illite; Ka = kaolinite; Kf = K-feldspar; Mu = muscovite; Pl= plagioclase; Sm = smectite; Ti = titanite. Open squares—basalts; solid circles—felsic rocks.

Ti, P, Th, Y and V) and rare earth elements (REE) in the mafic rocks remain constant over a wide range of CIA values, suggesting that these elements have been largely immobile during alteration. This evaluation is consistent with our petrographical observation that the mafic rocks only experienced lower greenschist facies metamorphism and chloritization during which the HFSE and REE are immobile (Morrison, 1978; Humphris and others, 1978). On the contrary, CaO, $Al_2O_3$ and the large ion lithophile elements (LILE, Sr, Rb) clearly correlate with CIA values, suggesting modification by alteration.

Most elements in the felsic rocks, except for LILE, show no correlation with CIA values (fig. 5), suggesting that they have been immobile during alteration. However, LILE such as $Na_2O$ and $K_2O$ show positive correlations with the CIA values, indicating mobilization during alteration. Therefore, we will use the immobile elements only in the following geochemical characterizations and petrogenetic discussions.

The Zhenzhushan volcanic rocks have a wide range of $SiO_2$ contents (49.11-73.73 wt.%), and display a bimodal distribution in the plot of $Zr/TiO_2$ versus Nb/Y (Winchester and Floyd, 1976) (fig. 6A). The basaltic rocks have $SiO_2$ (49.11-52.17 wt.%), MgO (7.89-10.26 wt.%), $FeO^t$ (11.70-13.29 wt.%), $P_2O_5$ ($\leq$0.13 wt.%) and $TiO_2$ (1.13-1.41 wt.%), and are Q-normative in CIPW norms. They have consistent Nb/Y ratios of 0.39 to 0.43, and plot exclusively in the subalkaline basalt field (fig. 5A). On F6

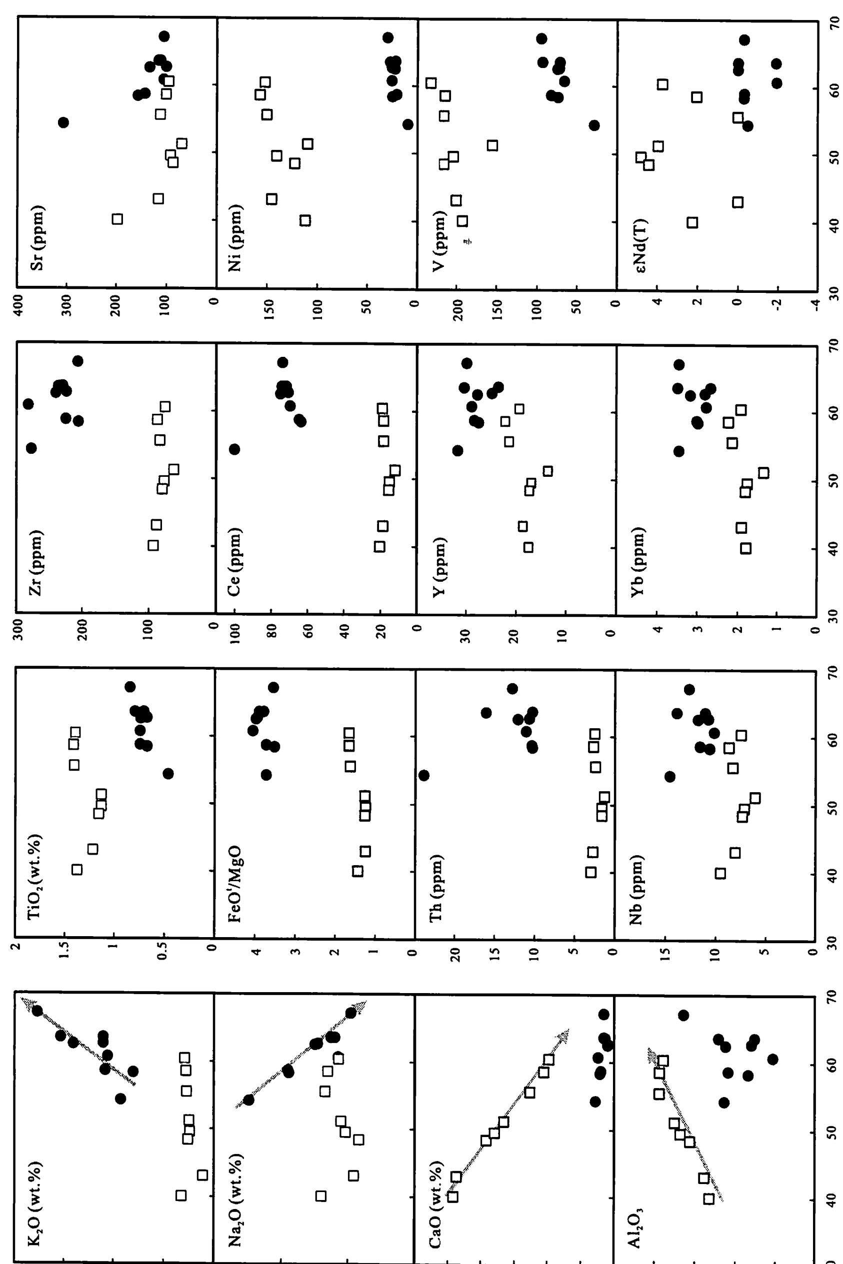


Fig. 5. Correlation diagrams of major and trace elements vs. CIA. Open squares—basalts; solid circles—felsic rocks.

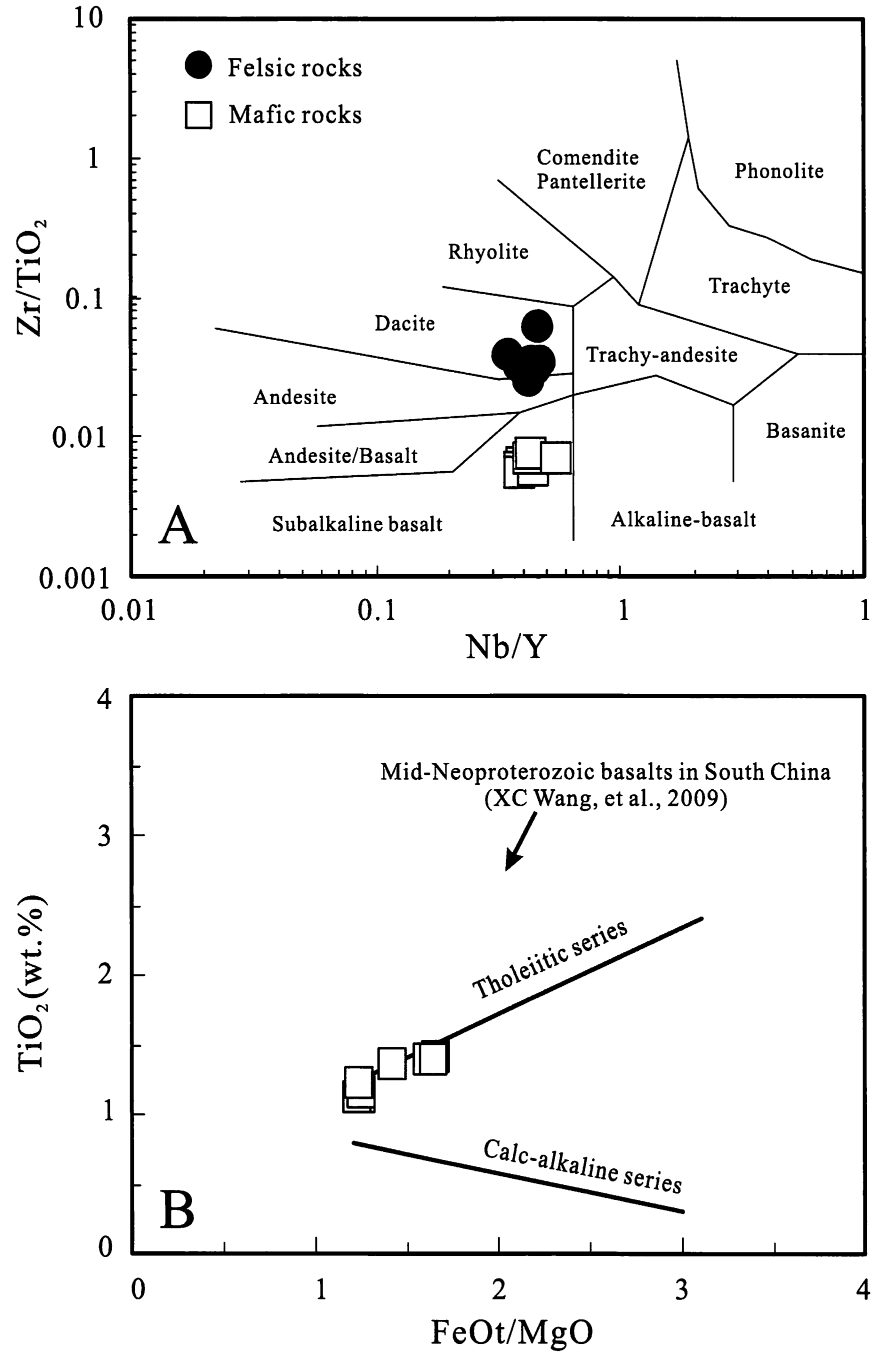


Fig. 6. (A) $Zr/TiO_2$ vs. Nb/Y diagram (Winchester and Floyd, 1976) for the classification of Zhenzhushan volcanic rocks. (B) $TiO_2$ vs. FeOt/MgO diagram of the mafic rocks of the Zhenzhushan Group, showing a tholeiitic series evolutionary trend. Symbols are as in figure 4.

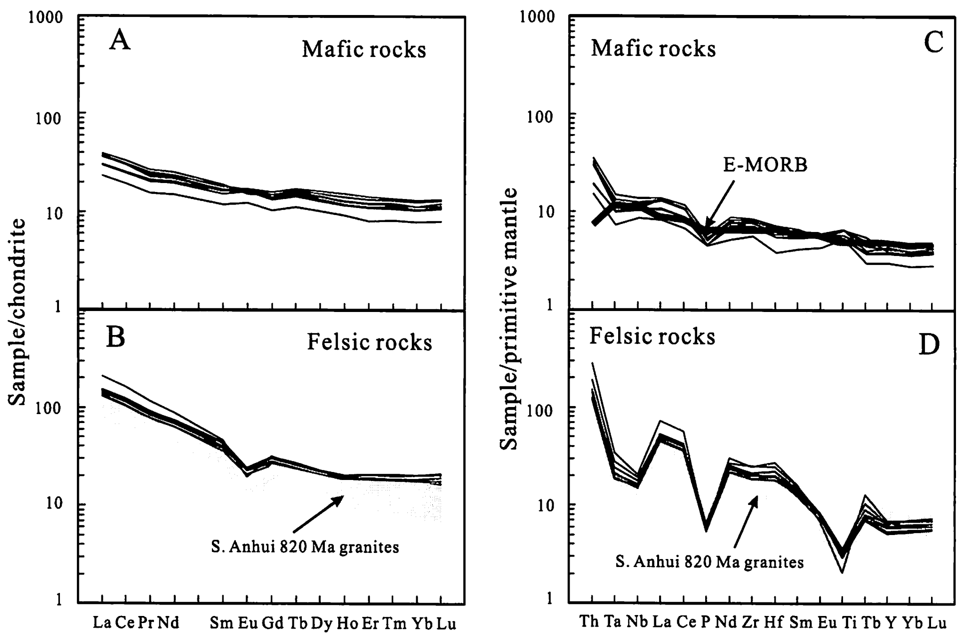


Fig. 7. Chondrite-normalized REE diagrams (A, B) and primitive mantle-normalized trace element diagrams (C, D) for the Zhenzhushan volcanic rocks. The data for the ca. 820 Ma southern Anhui granites are from X. H. Li and others (2003a). Normalization values are from Sun and McDonough (1989).

the $TiO_2$ versus $FeO^t/MgO$ diagram (fig. 6B) of Miyashiro (1974), their $TiO_2$ content increases with increasing $FeO^t/MgO$ ratio, defining a tholeiitic series evolutionary trend; they also fall into the mid-Neoproterozoic basaltic rock field for South China of (X. C. Wang and others, 2009). The felsic rocks have $SiO_2$ contents ranging from 67.6 to 73.7 weight percent and are peraluminous (ACNK = 1.2-2.1). Although the anomalously high ACNK values exceeding 2 (table 2) are most likely the results of subsequent alteration, the least-altered sample (06GDB05-7) also has a high ACNK value of 1.19. On the diagram of $Zr/TiO_2$ versus Nb/Y (fig. 6A), the felsic rocks plot mainly into the dacite field, but some overlap the boundary between andesite and dacite.

On the chondrite-normalized REE diagrams (fig. 7A), the basaltic samples show uniform and slightly LREE-enriched patterns with $La/Yb_N$ of 2.87 to 3.73, and slightly positive Eu anomalies ($\delta Eu$ = 1.03-1.13) with the exception of sample 06GDB04-8 with a weak negative anomaly ($\delta Eu$ = 0.91). In contrast, the felsic rocks have LREE-enriched patterns with $La/Yb_N$ of 7.2 to 10.3 and significant negative Eu anomalies ($\delta Eu$ = 0.51-0.74), similar to those of 820 Ma Neoproterozoic peraluminous granites in southern Anhui Province (fig. 7B). F7

On the primitive mantle-normalized trace elements diagrams (figs. 7C and 7D), the incompatible trace elements of the basaltic rocks are three- to ten-fold greater than that of the primitive mantle, and their patterns are similar to E-MORB type basalts but with negative P anomalies and positive Th anomalies relative to the neighboring elements. The felsic rocks display strongly fractionated patterns with significant negative Nb-Ta, P and Ti anomalies, also resembling those of the 820 Ma Neoproterozoic peraluminous granites in southern Anhui Province (fig. 7D).

TABLE 3

*Sm-Nd isotopic data for Zhenzhushan bimodal volcanic rocks*

| Sample # | Sm (ppm) | Nd (ppm) | $^{147}Sm/^{144}Nd$ | $^{143}Nd/^{144}Nd$ | $2\sigma_m$ | εNd(T) | $T_{DM}$(Ga) |
|---|---|---|---|---|---|---|---|
| **Felsic rocks** | | | | | | | |
| 06GDB03-1 | 5.52 | 29.58 | 0.1129 | 0.512154 | 0.000012 | -0.33 | 1.50 |
| 06GDB03-3 | 5.83 | 29.37 | 0.1199 | 0.512194 | 0.000010 | -0.32 | 1.55 |
| 06GDB03-4 | 6.80 | 34.74 | 0.1184 | 0.512185 | 0.000019 | -0.32 | 1.54 |
| 06GDB05-1 | 6.53 | 34.66 | 0.1140 | 0.512080 | 0.000006 | -1.90 | 1.63 |
| 06GDB05-5 | 6.93 | 36.63 | 0.1143 | 0.512080 | 0.000005 | -1.93 | 1.64 |
| 06GDB05-7 | 7.09 | 41.19 | 0.1041 | 0.512096 | 0.000012 | -0.50 | 1.46 |
| **Mafic rocks** | | | | | | | |
| 06GDB04-1 | 2.58 | 10.09 | 0.1544 | 0.512507 | 0.000007 | 2.05 | |
| 06GDB04-3 | 2.53 | 10.50 | 0.1456 | 0.512544 | 0.000019 | 3.74 | |
| 06GDB04-4 | 1.81 | 6.92 | 0.1584 | 0.512626 | 0.000006 | 3.93 | |
| 06GDB04-5 | 2.34 | 9.14 | 0.1549 | 0.512650 | 0.000006 | 4.79 | |
| 06GDB04-6 | 2.46 | 9.49 | 0.1569 | 0.512642 | 0.000008 | 4.40 | |
| 06GDB04-8 | 2.90 | 11.67 | 0.1500 | 0.512493 | 0.000007 | 2.24 | |

T = 850 Ma, formation age of Zhenzhushan volcanic rocks.

### *Nd Isotopic Geochemistry*

Twelve samples were selected for Nd isotope analysis, including six felsic rocks and six basaltic rocks, with analytical results listed in table 3. The basaltic rocks have relatively constant $^{147}Sm/^{144}Nd$ (0.146-0.158) and $^{143}Nd/^{144}Nd$ ratios (0.512493-0.512650), corresponding to εNd(T) values of 2.1 to 4.8, suggesting that they were derived from a long-term depleted mantle source. The felsic rocks have relatively lower $^{147}Sm/^{144}Nd$ (0.104-0.120) and $^{143}Nd/^{144}Nd$ ratios (0.512080-0.512194), corresponding to εNd(T) values of −0.32 to −1.93 and Nd model ages ($T_{DM}$) of 1.46 to 1.64 Ga. T3

## PETROGENESIS

### *Mafic Rocks*

Despite the Zhenzhushan basalts showing a relatively small range in $SiO_2$ (49.1-52.2 wt.%) and MgO (7.9-10.3 wt.%) contents, some major and trace element variations indicate that the magma underwent low-degree fractional crystallization. On the diagrams of Ni and Y versus Mg#, the basalts display two-stage evolution trends (figs. 8A and 8B). As Mg# decreases, the Ni abundance first drops from 145 to 109 ppm and then increases to 157 ppm, while the Y content first slightly increases and then shows a marked increase. These geochemical features indicate fractional crystallization in the magma of first olivine, then clinopyroxene and plagioclase (Wilson, 1989; Kerr and others, 1997). The slight increase in $TiO_2$ abundance from ~1.1 weight percent to 1.4 weight percent and generally constant $Fe_2O_3$ abundance of 12 to 13 weight percent (table 2) suggest that Fe-Ti oxides were probably not fractionated from the magma, consistent with that of typical tholeiitic basalts (Wilson, 1989). F8

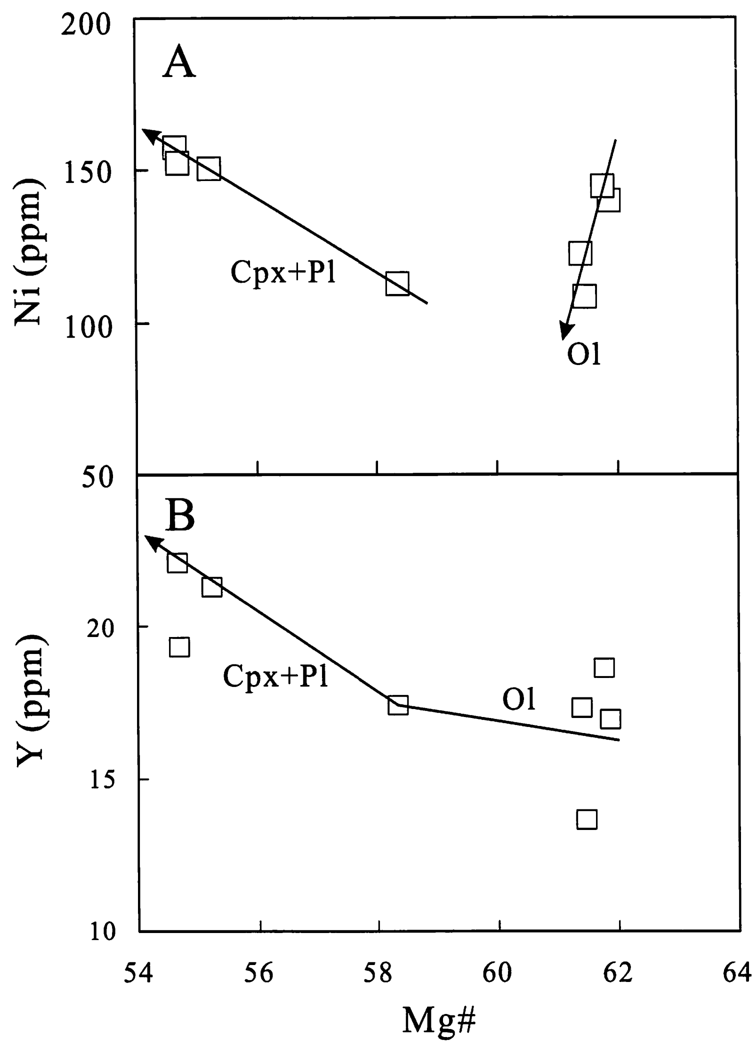


Fig. 8. Plots of (A) Ni vs. MgO# and (B) Y vs. MgO# showing that the Zhenzhushan basalts underwent fractional crystallization of olivine first and then clinopyroxene and plagioclase. Symbols are as in figure 4.

The Zhenzhushan basalts have low Nb/Th (3-4.8) and variable Nb/U (19.3-48.7) ratios in comparison to primitive mantle values (Nb/Th=8.4; Nb/U=34, Sun and McDonough, 1989), suggesting source or crustal contamination. However, the basalts show positive correlation between Nb/Th and Nb/U with Nb/La (figs. 9A and 9B). F9 Together with the negative correlation between εNd(T) and MgO abundance (fig. 9C), this indicates that crustal contamination played an important role.

Despite experiencing fractional crystallization of different minerals and variable crustal contamination, the basalts exhibit overall incompatible trace element patterns similar to those of intraplate basalts, rather than volcanic arc rocks (fig. 10). They have F10 positive εNd(T) values of 2.1 to 4.8 and E-MORB-like trace element patterns (fig. 10). Except for the obvious Th enrichment due to crustal contamination, all these suggest that the basalts were likely derived from a depleted asthenosphere mantle source (X. H. Li and others, 2008). In addition, the basalts are characteristically high in Ti, V

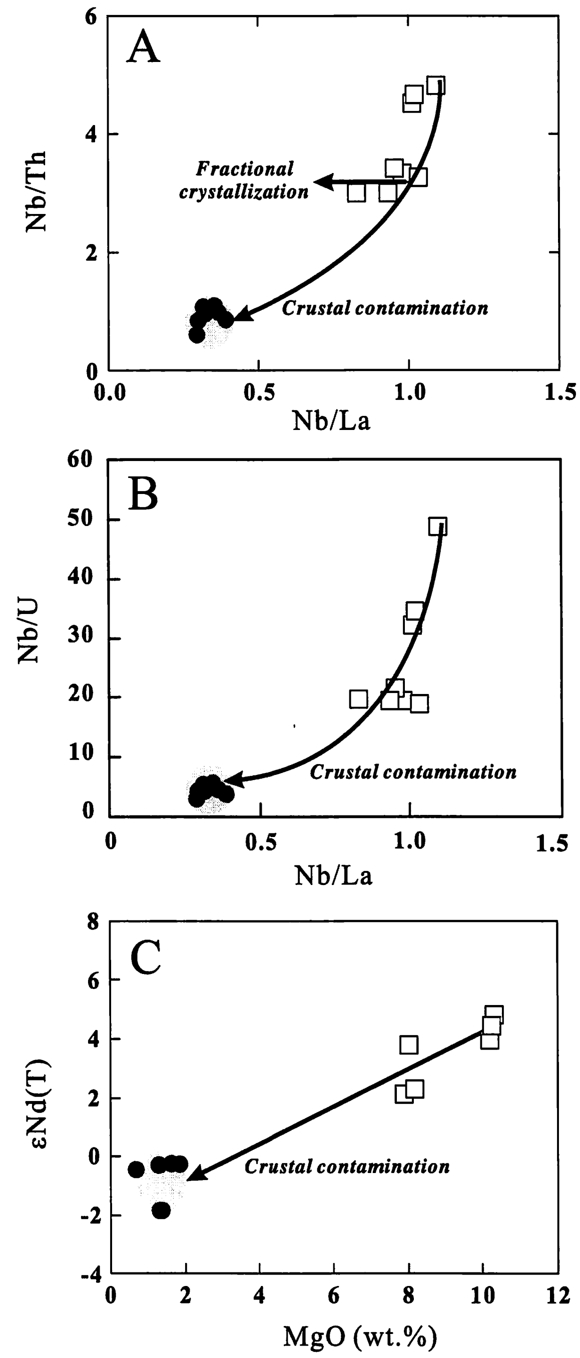


Fig. 9. Plots of (A) Nb/Th vs. Nb/La, (B) Nb/U vs. Nb/La and (C) εNd(T) vs. MgO showing trends of contamination by crustal materials (possibly associated felsic volcanic rocks). Symbols are as in figure 4.

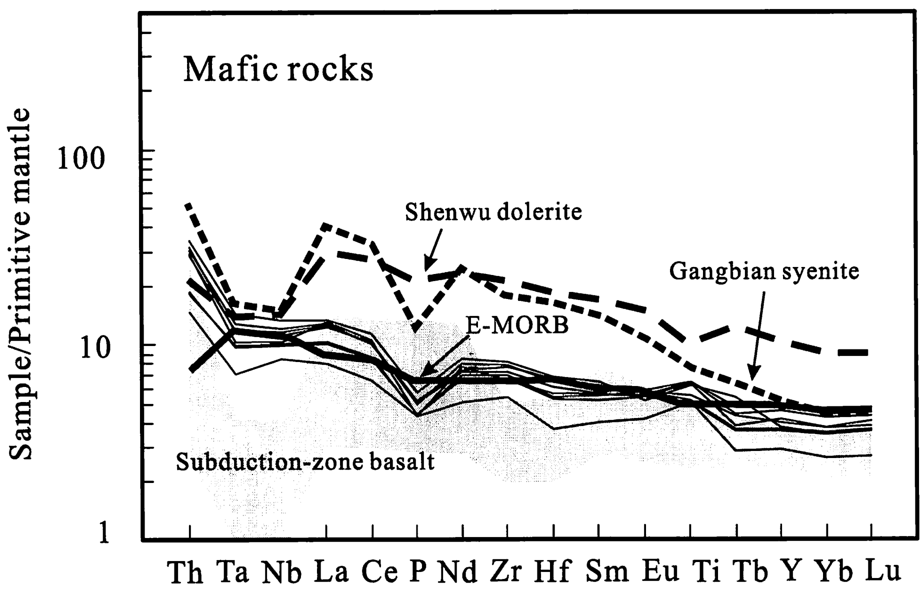


Fig. 10. Comparison of primitive mantle-normalized incompatible trace element spider diagrams for the Zhenzhushan basalts with those of E-MORB basalts (Sun and McDonough, 1989), the average value of the Shenwu mafic dykes (X. H. Li and others, 2008), and the average value of the Ganbian alkaline syenite (X. H. Li and others, 2010). The shaded area shows the range for subduction zone basalts, with the lower and upper limits being defined by "average" low-K and high-K basalts, respectively (Tatsumi and Eggins, 1995).

and Zr, but low in Y, comparable with within-plate basalts (figs. 11A and 11B). On the Ti-Sm-V discrimination diagram of Vermeesch (2006), which has been proved to be the best quadratic tectonic discrimination diagram using immobile trace elements for basaltic rocks, the basalts plot within the oceanic island basalt (OIB) and mid-ocean ridge basalt (MORB) fields (fig. 11C). Therefore, the Zhenzhushan basalts were likely formed in an extension-related, rather than subduction-related tectonic environment. F11

It is noted that the Zhenzhushan basalts are Si-saturated tholeiites in composition. Such quartz-tholeiites may be generated by high degree anhydrous partial melting of a depleted mantle source at low pressures, possibly at the top of an asthenospheric upwelling (Gibson and others, 1993). However, such basalts should have high alumina (17-18 wt.%, Jaques and Green, 1980). The $Al_2O_3$ contents of the least-evolved Zhenzhushan basalts (Mg# > 60), on the other hand, are generally below 17 weight percent (table 2), indicating that the primitive magma may have been low in $Al_2O_3$. Therefore, high degree anhydrous partial melting of a depleted mantle source at low pressure is not the best model for the formation of the basalts.

The concentration of $SiO_2$ may be increased by hydrous partial melting of mantle peridotite, because the presence of $H_2O$ expands the olivine stability field, causing the melt to become silica saturated (Mysen and Boettcher, 1975). This is believed to have taken place in the Cenozoic Rio Grande Rift of the western USA, where some quartz-tholeiitic basalts originated in the axial part of the rift (Gibson and others, 1993). Water contents in the asthenosphere beneath the Rio Grande Rift were interpreted to have been enhanced by the previous subduction of the Farallon plate. Similarly, water contents beneath the southeastern margin of the Yangtze Block could have been elevated by oceanic subduction during the pre-890 Ma Sibao orogenic event (Z. X. Li and others, 2002, 2007; X. H. Li, and others, 2009a). Therefore, we regard hydrous partial melting of the asthenospheric mantle as the best model for the formation of the Zhenzhushan basalts.

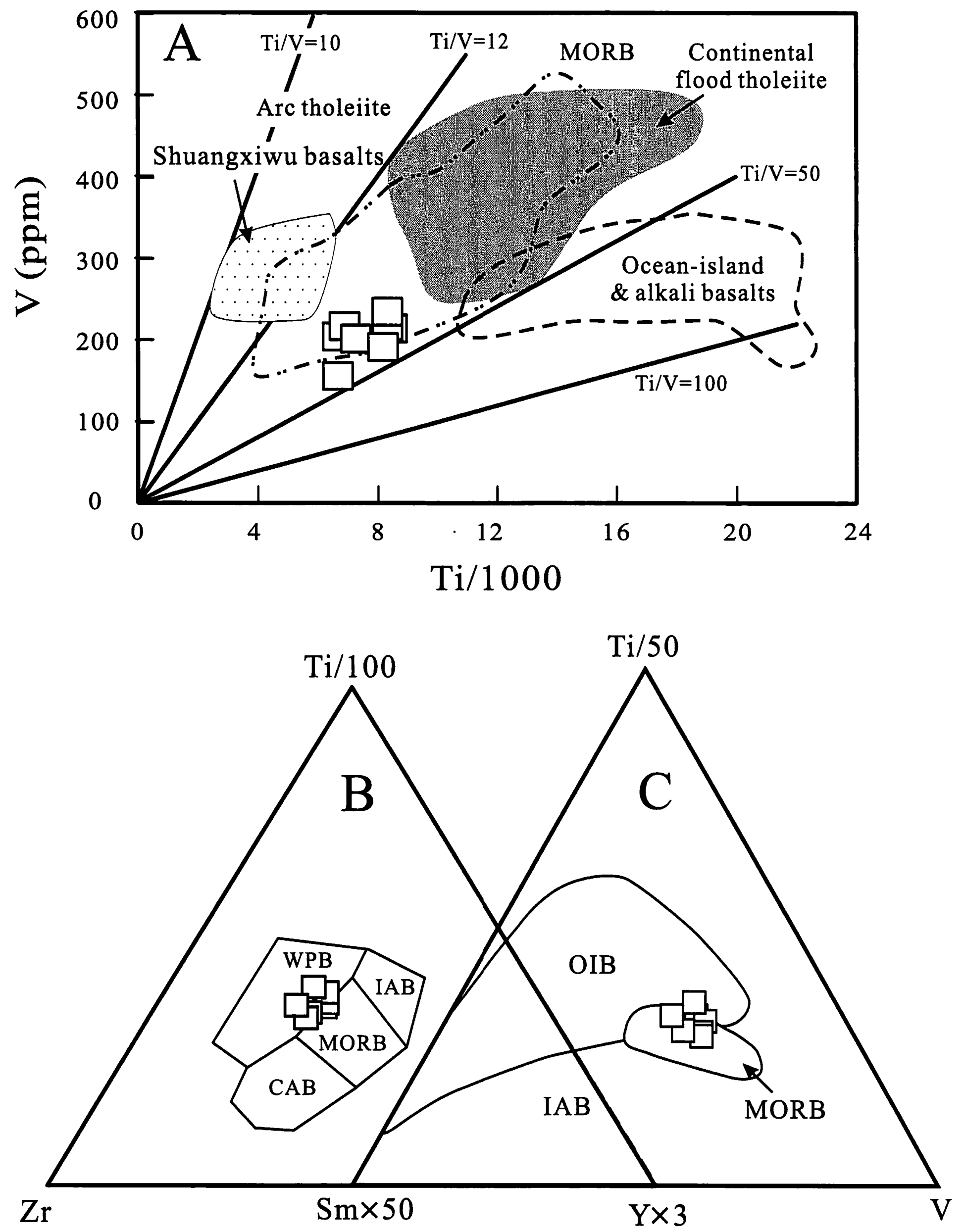


Fig. 11. Tectonic discrimination plots for the Zhenzhushan basalts. (A) V versus Ti/1000 plot of Shervais (1982). The fields of arc tholeiite, mid-ocean-ridge basalt (MORB), continental flood basalt, and ocean-island and alkali basalt follow Rollinson (1993). The field for the Shuangxiwu basalts is from X. H. Li and others (2009a). (B) Ti-Zr-Y (Pearce and Cann, 1973) and (C) Ti-Sm-V (Vermeesch, 2006) diagrams showing that the Zhenzhushan basalts plot in the OIB or MORB field, suggesting their formation in an extensional tectonic environment. Symbols are as in figure 4.

### *Felsic Rocks*

The origin of the felsic volcanic rocks in the bimodal igneous suites is often debated. Two major geological processes may lead to the production of felsic magma:

(1) partial melting of crustal materials during the same thermal event that produces coeval basaltic magma (Suneson and Lucchita, 1983; X. H. Li and others, 2002); (2) assimilation of crustal materials by ascending mantle-derived basaltic magmas through AFC processes (Peccerillo and others, 2003). There are different trends between the Zhenzhushan felsic and mafic rocks in their Th, Ce and Zr versus Nb plots (fig. 12) and they have distinct Nd isotopic characteristics (table 3), suggesting that the felsic rocks were unlikely formed by AFC processes of coeval basaltic magma (Wilson, 1989; Pin and Paquette, 1997). These felsic rocks are characteristically high in $SiO_2$ and $Al_2O_3$, with ACNK values ranging from 1.19 to 2.05, belonging to the peraluminous series. The Nd isotopic characteristics of the felsic rocks are similar to those of the Neoproterozoic (ca. 820 Ma) peraluminous granites in the southern Anhui and northern Jiangxi regions, which have been interpreted to have originated from partial melting of crustal materials (X. H. Li and others, 2003a; Wu and others, 2006). Considering that they have εNd(t) of −0.3 to −1.9, we suggest that they were likely formed by partial melting of Mesoproterozoic/early Neoproterozoic immature sedimentary rocks deposited in a continental margin or back-arc basin (X. H. Li and others, 2003a; Wu and others, 2006). F12

*Ca. 850 Ma Continental Rifting Along the Southeastern Margin of the Yangtze Block*

Ca. 850 Ma magmatic rocks are rare in South China, and the tectonic significance of those rocks is unclear. X. L. Wang and others (2008) reported a ~880 Ma zircon age for a felsic unit interlayered in the Shuangqiaoshan Group in NE Jiangxi (marked as 4 in fig. 1A), and they interpreted that the 880 to 850 Ma volcanic units of the Shuangqiaoshan Group were formed in a back-arc basin. This interpretation contradicts that of X. H. Li and others (2009a) that calc-alkaline volcanic arc magmatism along the southeastern Yangtze Block ceased at ~890 Ma. W. X. Li and others (2008a) reported a ~880 Ma obduction-type granite within the ~1000 Ma NE Jiangxi ophiolite between the Yangtze and Cathaysia blocks in eastern South China (Chen and others, 1991), suggesting that the back arc basin was closed by ~880 Ma. This is consistent with the 1042 to 1015 Ma and 970 to 940 Ma orogenic-related metamorphic events as reported by Z. X. Li and others (2007) from this region. We note the presence of a ca. 770 Ma zircon age population in two of the samples analyzed by X. L. Wang and others (2008), including the sample from the supposedly 880 Ma volcanic unit (three spots from sample SQS-03 and seven spots from sample SQS-08-1; see table 2 and fig. 6 of X. L. Wang and others, 2008), indicating that the Shuangqiaoshan rocks were probably no older than 770 Ma, not ca. 880 Ma as those authors interpreted. In addition, their analyzed ca. 880 Ma zircons are characterized by high εHf(t) values of 3.3 to 18.8, similar to those of the volcanic and intrusive rocks in the neighboring Shuangxiwu arc. This suggests that the older zircons were possibly derived from the erosion of the Shuangxiwu arc (X. H. Li and others, 2009a).

X. H. Li and others (2008, 2010) reported a ~850 Ma age for the Gangbian alkaline complex in NE Jiangxi Province (marked as 2 in fig. 1A) and a ~850 Ma age for the intraplate Shenwu dolerite dike in central Zhejiang Province (marked as 3 in the fig. 1A). They considered that the ~850 Ma magmatism in eastern South China occurred in an anorogenic setting related to either a post-orogenic event or the onset of Neoproterozoic continental rifting. A rifting model would predict the possible existence of bimodal volcanic rocks in the region.

Our new data for the Zhenzhushan bimodal volcanic rocks, with basalts showing E-MORB-like geochemical features, for the first time demonstrate the presence of ca. 850 Ma bimodal volcanic rocks in eastern South China, thus lending further support to the continental rift model. Apart from the 848 ± 4 Ma Gangbian alkaline complex and the 849 ± 7 Ma Shenwu doleritic dyke mentioned above, coeval magmatism in the southeastern Yantzge Block also includes the 838 ± 5 Ma and 841 ± 6 Ma Chencai

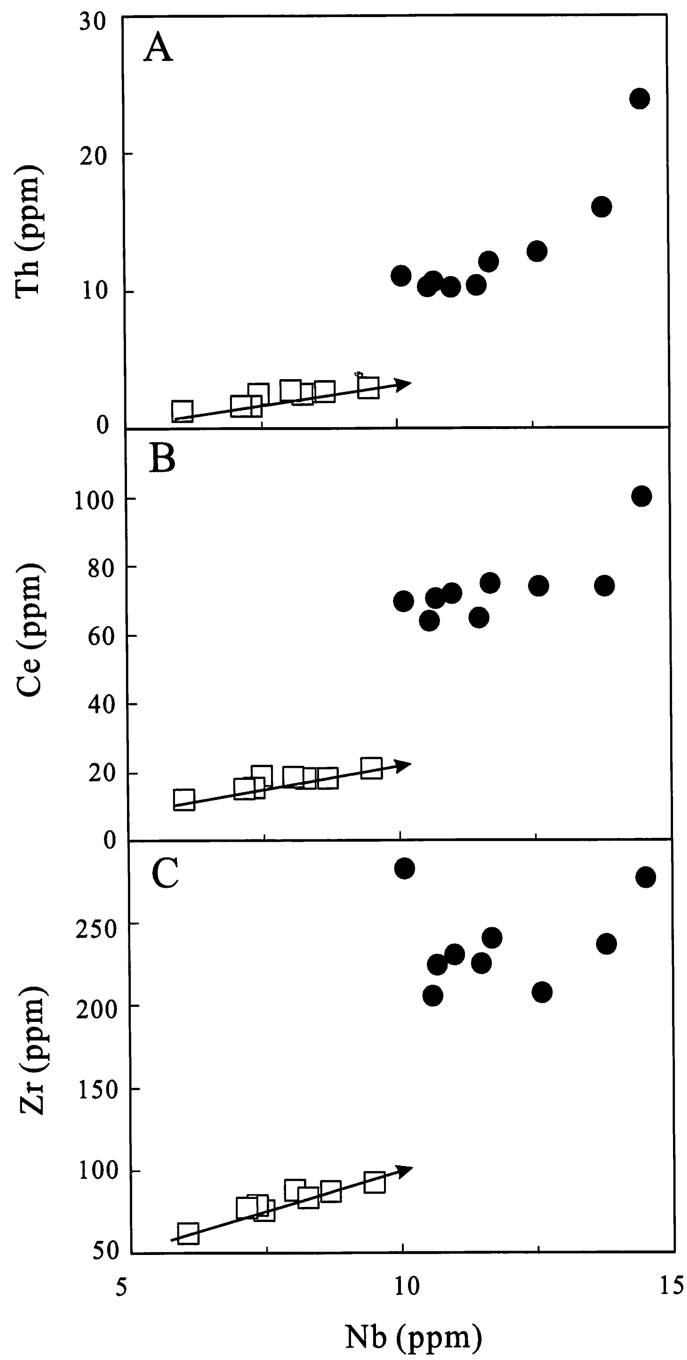


Fig. 12. Plots of (A) Th vs. Nb; (B) Ce vs. Nb and (C) Zr vs. Nb showing different evolutionary trend for mafic and felsic rocks, implying that there is not a petrogenetic relation between them. Symbols are as in figure 4.

bimodal volcanic rocks and the Lipu dioritic pluton in central Zhejiang (Z. X. Li and others, 2010, marked as 1 in fig. 1A). Geochemical data for the Chencai volcanic rocks and the Lipu diorites are not available, but data from the other, roughly coeval mafic

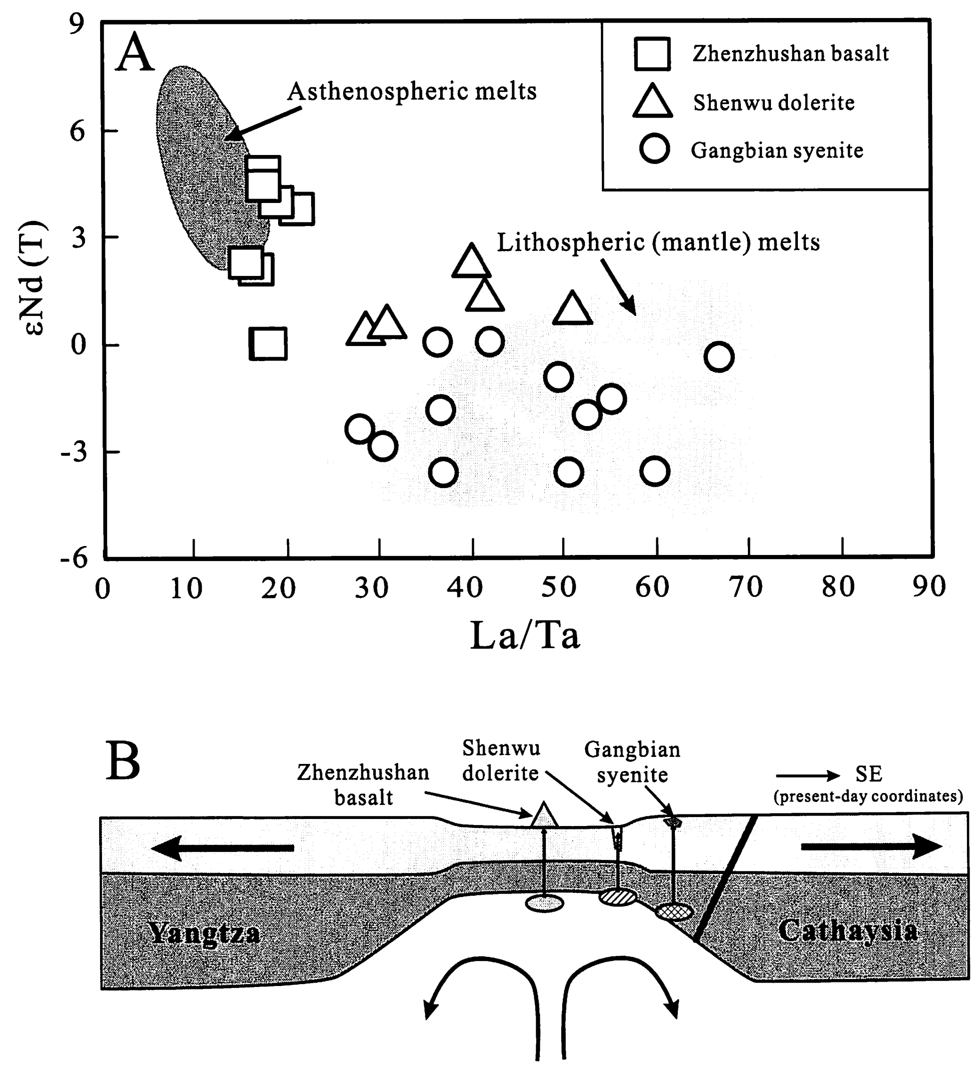


Fig. 13. (A) Plot of εNd(T) vs. La/Ta for the Zhenzhushan basalts. The fields of asthenospheric melts and arc magmatic rocks are from Lawton and others (1999). Data sources: Shenwu dolerite from X. H. Li (2008); Gangbian syenite from X. H. Li (2010). (B) Cartoon showing the extension/rifting of the South China lithosphere at ca. 850 Ma due to the arrival of warm mantle return flow probably derived from the Rodinia superplume (Z. X. Li, 2008).

and alkaline rocks show a clear change in their sources from a metasomatic lithospheric mantle in the southeast to an asthenospheric mantle in the northwest, as demonstrated by their εNd(T) versus La/Ta values (fig. 13A), suggesting a lateral transition from a rift shoulder in the southeast to the rift axis in the northwest (fig. 13B). This is similar to that in the Cenozoic Rio Grande Rift of the western USA, where the lithospheric mantle-derived K-enriched alkaline rocks occur along the flank of the rift, while the asthenospheric mantle-derived tholeiitic basalts are in the axis of the rift (Gibson and others, 1993). F13

Other 870 to 830 Ma magmatic rocks in the South China Block include the 836 ± 3 Ma Zhaigu granite (X. L. Wang and others, 2006; marked as 5 in fig. 1A), the 857 ±

13 Ma Guandaoshan diorite (marked as 6 in fig. 1A; X. H. Li and others, 2003b) and the 844 ± 2 Ma Fangcheng syenite (marked as 7 in fig. 1A; Bao and others, 2008), all interpreted as of anorogenic origin. Possible coeval sedimentary sequences are spread from the southeastern to the central part of the South China Block, including the Lengjiaxi Group in Hunan, the Sibao Group in northern Guangxi and the Fanjingshan Group in northern Guizhou. Sedimentary rocks from the Lengjiaxi Group contain abundant 870 to 860 Ma detrital zircons (X. L. Wang and others, 2007; marked as 10 in the fig. 1A). In northern Guangxi and Guizhou, the Sibao and Fanjingshan groups that underlie the ca. 820 Ma rift-related sequences also contain abundant 870 to 860 Ma detrital zircons (X. L. Wang and others, 2007; J. C. Zhou and others, 2009; marked as 11 and 12, respectively, in fig. 1A). It is noted that all these rocks are located within or close to the 825 to 750 Ma continental rift systems in South China (for example, Z. X. Li and others, 1999, 2003; X. H. Li and others, 2003a; Wang and Li, 2003). It is therefore possible that the ca. 850 rifting event represents the early onset of subsequent, more extensive rifting events.

Possible 850 to 830 Ma magmatic and sedimentary rocks in South China have also been interpreted as being formed in a back-arc basin or a foreland basin (X. L. Wang and others, 2007, 2008; J. C. Zhou and others, 2009). Zhou and others (2009) recently reported 822 ± 15 Ma basalts and ca. 870 Ma detrital zircons from the Fanjingshan Group in northern Guizhou Province (marked as 12 in fig. 1A), and interpreted the rocks to be of arc origin possibly formed in a foreland basin between 870 and 820 Ma. However, we notice that the reported basalts have high Nb/Y ratio (1.2-2.4), making them alkaline basalts rather than calc-alkaline basalts as the authors believed. In addition, these basalts show no Zr and Hf depletion relative to Sm (as in figure 8c-d of Zhou and others, 2009), unlike typical arc basalts (for example, McCulloch and Gamble, 1991). The negative Nb-Ta anomalies (so-called "arc-signatures") in the Fanjingshan basalts are thus likely the results of crustal or sub-continental lithospheric mantle contamination (X. H. Li and others, 2007). We illustrate in figure 14 our preferred interpretation for the tectonic evolution of the southeastern Yangtze Block during the early-middle Neoproterozoic, featuring a switch in tectonic regime from the end of the Sibao Orogeny at ca. 880 Ma (W. X. Li and others, 2008a) to the start of continental rifting by ca. 850 Ma (X. H. Li and others, 2010; this study). F14

### *An Early Episode of Continental Extension and Rifting Related to the Break-Up of the Supercontinent Rodinia*

If our interpretation of the ca. 850 Ma onset of continental rifting in South China is correct, it would imply that continental rifting that led-up to the breakup of the supercontinent Rodinia started at least ca. 30 Ma earlier than the well-documented ca. 820 Ma age, and less than 50 Ma after its final assembly (ca. 900 Ma, Z. X. Li and others, 2008). Similar to South China, early rift-related magmatism is also reported in other parts of Rodinia. In the Scottish promontory of Laurentia, the ca. 870 Ma Knoydartian "Orogeny" has been interpreted by some as representing an extensional event (Soper and others, 1998; Dalziel and Soper, 2001) and Z. X. Li and others (2008) speculated it may represent the first surface expression of the Rodinia superplume. The presence of abundant ~870 Ma MORB-like basaltic dikes and anatectic granites in the same region (Friend and others, 1997; Millar, 1999) is consistent with such an interpretation. In the Zambezi Belt along the southern margin of the Congo Craton, ca. 870 Ma felsic volcanic rocks ~2500 m thick were interpreted as being formed in a continental rift setting (Johnson and others, 2005, 2007; De-Waele and others, 2008). In the Seve-Kalak Superterrane derived from the margin of the Baltica Block, ca. 850 Ma granites were interpreted as being formed by anatexis during the emplacement of gabbros into metasedimentary rocks in an extensional environment (Paulsson and Andreasson, 2002). In Arctic Alaska, ca. 870 Ma intermediate to felsic volcanic rocks in the

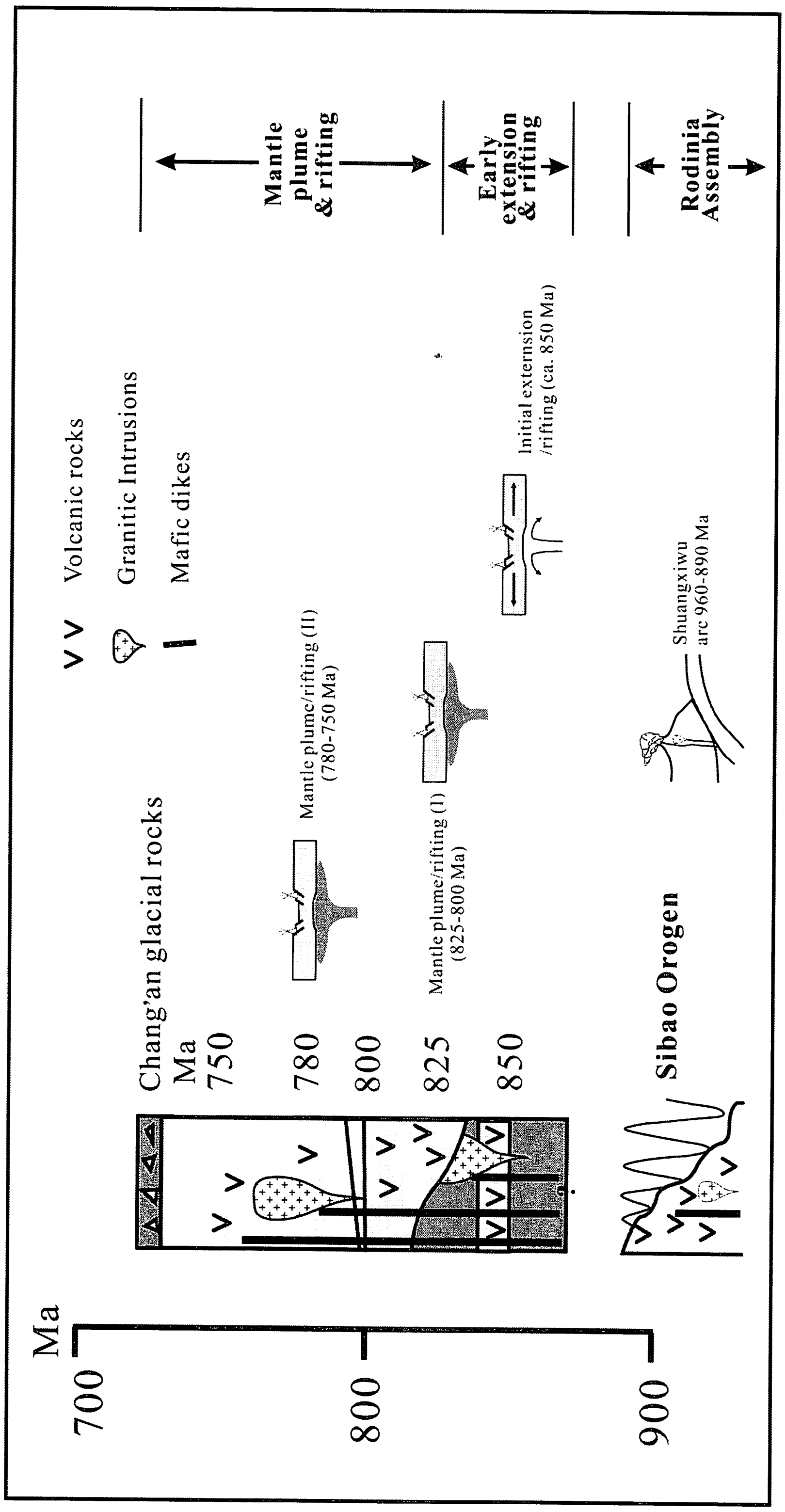


Fig. 14. (A) Schematic tectonostratigraphic diagram for the southeastern Yangtze Block showing multiple-phases of extension and rift events between 900 Ma and 700 Ma (modified after Z. X. Li and others, 2008).

Chukotka terrane were also considered to be related to the initial break-up of the supercontinent Rodinia (Amato and others, 2009). Dalziel and Soper (2001) and Paulsson and Andreasson (2002) interpreted the 870 to 850 Ma magmatism as being related to the initial breakup of the supercontinent Rodinia with rifting along the northern margin of Laurentia. It is thus possible that extensive Rodinia-wide continental extension and rifting started only 30 to 50 Ma after the final assembly of the supercontinent at ca. 900 Ma (Z. X. Li and others, 2008), which is ca. 30 to 50 Ma earlier than the first well-documented mantle plume event at ca. 825 Ma (for example, Z. X. Li and others, 1999, 2003, 2008; X. C. Wang and others, 2007). We interpret the 870 to 830 Ma extension event to reflect the early arrival of warm mantle underneath the supercontinent as a result of circum-supercontinent mantle avalanches (Z. X. Li and others, 2004, 2008; Zhong and others, 2007; Li and Zhong, 2009).

## CONCLUSIONS

High precision SIMS U-Pb zircon dating indicates that the Zhenzhushan felsic volcanic rocks were formed at 849 ± 6 Ma, significantly younger than the ca. 1000 to 890 Ma Shuangxiwu arc and the 1042 to 1015 and 970 to 940 Ma orogenic-related metamorphic events that were recorded in the same region. The ~850 Ma magmatic event reported here is older than the more extensive 820 to 750 Ma plume-related bimodal magmatism in the region. Our geochemical analyses show that the Zhenzhushan basalts are $SiO_2$-saturated tholeiitic rocks probably generated by high-degrees of partial melting of hydrous, depleted mantle in an extensional environment, with the magma experiencing fractional crystallization and crustal contamination. The associated felsic rocks were possibly formed by partial melting of Mesoproterozoic/early Neoproterozoic sedimentary rocks. Combined with available results from contemporary alkaline complexes and mafic dikes in the southeastern margin of the Yangtze Block, we conclude that the Zhenzhushan bimodal volcanic rocks were probably formed in the axial region of a ca. 850 Ma continental rift during the early stage of widespread Neoproterozoic continental rifting. This event occurred 30 to 50 Ma after the amalgamation of the Yangtze and Cathaysia blocks, and ca. 30 Ma earlier than the first known Neoproterozoic mantle plume event in South China. Coeval ca. 850 Ma anorogenic magmatism has also been reported in other parts of Rodinia, possibly reflecting initial rifting within the supercontinent Rodinia related to the formation of the Rodinia superplume that eventually broke-up the supercontinent.

## ACKNOWLEDGMENTS

We would like to thank Y. Liu, X. L. Tu, and X. R. Liang for their assistance in geochemical and Nd isotopic analyses, and Y. Liu and G. Q. Tang for SIMS U-Pb zircon analyses. H. Q. Huang is thanked for help in the field. Review comments by Professors S. L. Chung and M. Sun, and that of Guest Editor Professor S. A. Wilde, helped to improve the manuscript. This work was supported by the Chinese Academy of Sciences (KZCX2-YW-Q08-4, KZCX1-YW-15-2 and KZCX2-YW-128), NSFC (grants 40721063 and 40573016), the Australian Research Council (DP0770228) and the Institute for Geoscience Research (TIGeR). This work was also jointly supported by a research grant from the State Key Laboratory of Lithospheric Evolution, Institute of Geology and Geophysics, Chinese Academy of Sciences. This is contribution No. IS-1256 from GIGCAS and TIGeR publication #237.

## REFERENCES

Amato, J. M., Toro, J., Miller, E. L., Gehrels, G. E., Farmer, G. L., Gottlieb, E. S., and Till, A. B., 2009, Late Proterozoic-Paleozoic evolution of the Arctic Alaska-Chukotka terrane based on U-Pb igneous and detritial zircon ages: Implications for Neoproterozoic paleogeographic reconstructions: Geological Society of America Bulletin, v. 121, p. 1219–1235, doi: 10.1130/B26510.1.

Bao, Z. W., Wang, Q., Bai, G. D., Zhao, Z. H., Song, Y. W., and Liu, X. M., 2008, Geochronology and geochemistry of the Fangcheng Neoproterozoic alkali-syenites in East Qinling orogen and its geodynamic implications: Chinese Science Bulletin, v. 53, n. 13, p. 2050–2061, doi: 10.1007/s11434-008-0113-z.

Black, L. P., Kamo, S. L., Allen, C. M., Aleinikoff, J. N., Davis, D. W., Korsch, R. J., and Foudoulis, C., 2003, TEMORA 1: a new zircon standard for Phanerozoic U-Pb geochronology: Chemical Geology, v. 200, p. 155–170, doi: 10.1016/S0009-2541(03)00165-7.

Chen, J., Foland, K. A., Xing, F., Xu, X., and Zhou, T., 1991, Magmatism along the southeastern margin of the Yangtze block: Precambrian collision of the Yangtze and Cathaysia blocks of China: Geology, v. 19, p. 815–818, doi: 10.1130/0091-7613(1991)019<0815:MATSMO>2.3.CO;2.

Cheng, H., 1991, The late Proterozoic collision orogen in northwestern Zhejiang Province: Geological Review, v. 3, p. 203–213 (in Chinese with English Abstract).

—— 1993, Geochemistry of Proterozoic island-arc volcanic rocks in Northwest Zhejiang: Geochimica, v. 22, p. 18–27 (in Chinese with English Abstract).

Dalziel, I. W. D., 1991, Pacific margins of Laurentia and east Antarctica-Australia as conjugate rift pair: Evidence and implications for an Eocambrian supercontinent: Geology, v. 19, p. 598–601, doi: 10.1130/0091-7613(1991)019<0598:PMOLAE>2.3.CO;2.

Dalziel, I. W. D., and Soper, N. J., 2001, Neoproterozoic extension on the Scottish Promontory of Laurentia: Paleogeographic and Tectonic Implications: The Journal of Geology, v. 109, p. 299–317, doi: 10.1086/319974.

De Waele, B. D., Johnson, S. P., and Pisarevsky, S. A., 2008, Palaeoproterozoic to Neoproterozoic growth and evolution of the eastern Congo Cration: Its role in the Rodinia puzzle: Precambrian Research, v. 160, p. 127–141, doi: 10.1016/j.precamres.2007.04.020.

Deng, G., Lou, F., and Huang, C., 2003, Establishment of the Zhenzhushan Group in northeast Jiangxi and its significance: Geological Bulletin of China, v. 22, n. 1, p. 32–42 (in Chinese with English abstract).

Friend, C. R. L., Kinny, P. D., Rogers, G., Strachan, R. A., and Paterson, B. A., 1997, U-Pb zircon geochronological evidence for Neoproterozoic events in the Glenfinnan Group (Moine Supergroup): the formation of the Ardgour granite gneiss, north-west Scotland: Contributions to Mineralogy and Petrology, v. 128, p. 101–113, doi: 10.1007/s004100050297.

Gibson, S. A., Thompson, R. N., Leat, P. T., Morrison, M. A., Hendry, G. L., Dickin, A. P., and Mitchell, J. G., 1993, Ultrapotassic magmas along the flanks of the Oligo-Miocene Rio Grand Rift, USA: Monitors of the zone of lithospheric mantle extension and thinning beneath a continental rift: Journal of Petrology, v. 34, p. 187–228, doi: 10.1093/petrology/34.1.187.

Hoffman, P. F., 1991, Did the breakout of Laurentia turn Gondwanaland inside-out?: Science, v. 252, p. 1409–1412, doi: 10.1126/science.252.5011.1409.

Humphris, S. E., Morrison, M. A., and Thompson, R. N., 1978, influence of rock crystallization history upon subsequent Lanthanide Mobility during hydrothermal alteration of basalts: Chemical Geology, v. 23, p. 125–137, doi: 10.1016/0009-2541(78)90070-0.

Jaques, A. L., and Green, D. H., 1980, Anhydrous melting of peridotite at 0–15 kb pressure and the genesis of tholeiitic basalts: Contributions to Mineralogy and Petrology, v. 73, p. 287–310, doi: 10.1007/BF00381447.

Johnson, S. P., Rivers, T., and De Waele, B., 2005, A review of the Mesoproterozoic to early Palaeozoic magmatic and tectonothermal history of south-central Africa: implications for Rodinia and Gondwana: Journal of the Geological Society, London, v. 162, p. 433–450, doi: 10.1144/0016-764904-028.

Johnson, S. P., De Waele, B., Evans, D., Banda, W., Tembo, F., Milton, J. A., and Tani, K., 2007, Geochronology of the Zambezi Supercrustal sequence, southern Zambia: A record of Neoproterozoic divergent processes along the Southern Margin of the Congo Craton: Journal of Geology, v. 115, p. 355–374, doi: 10.1086/512757.

Kerr, A. C., Tarney, J., Marriner, G. F., Nivia, A., and Saunders, A. D., 1997, The Caribbean-Colombian Cretaceous Igneous Province: the internal anatomy of an Oceanic Plateau, *in* Mahoney, J. J., and Coffin, M. F., editors, Large Igneous Provinces-continental, oceanic, and planetary flood volcanism: American Geophysical Union Monograph, v. 100, p. 123–144.

Lawton, T. F., and McMillan, N. J., 1999, Arc abandonment as a cause for passive continental rifting: Comparison of the Jurassic Mexican Borderland rift and the Cenozoic Rio Grande rift: Geology, v. 27, p. 779–782, doi: 10.1130/0091-7613(1999)027<0779:AAAACF>2.3.CO;2.

Li, Q. L., Li, X. H., Liu, Y., Tang, G. Q., Yang, J. H., and Zhu, W. G., 2010, Precise U-Pb and Pb-Pb dating of Phanerozoic baddeleyite by SIMS with oxygen flooding technique: Journal of Analytical Atomic Spectrometry, v. 25, p. 1107–1113, doi: 10.1039/b923444f.

Li, W. X., and Li, X. H., 2003, Adakitic granites within the NE Jiangxi ophiolites, South China: geochemical and Nd isotopic evidence: Precambrian Research, v. 122, p. 29–44, doi: 10.1016/S0301-9268(02)00206-1.

Li, W. X., Li, X. H., and Li, Z. X., 2005, Neoproterozoic bimodal magmatism in the Cathaysia Block of South China and its tectonic significance: Precambrian Research, v. 136, p. 51–66, doi: 10.1016/j.precamres.2004.09.008.

Li, W. X., Li, X. H., Li, Z. X., and Lou, F. S., 2008a, Obduction-type granites within the NE Jiangxi Ophiolite: Implications for the final amalgamation between the Yangtze and Cathaysia Blocks: Gondwana Research, v. 13, p. 288–301, doi: 10.1016/j.gr.2007.12.010.

Li, W. X., Li, X. H., and Li, Z. X., 2008b, Middle Neoproterozoic syn-rifting volcanic rocks in Guangfeng, South China: petrogenesis and tectonic significance: Geological Magazine, v. 145, p. 475–489, doi: 10.1017/S0016756808004561.

Li, X. H., Sun, M., Wei, G. J., Liu, Y., Lee, C. Y., and Malpas, J. G., 2000, Geochemical and Sm-Nd isotopic study of amphibolites in the Cathaysia Block, southeastern China: evidence for extremely depleted mantle in the Paleoproterozoic: Precambrian Research, v. 102, p. 251–262, doi: 10.1016/S0301-9268(00)00067-X.

Li, X. H., Li, Z. X., Zhou, H., Liu, Y., and Kinny, P. D., 2002, U-Pb zircon geochronology, geochemistry and Nd isotopic study of Neoproterozoic bimodal volcanic rocks in the Kangdian Rift of South China: implications for the initial rifting of Rodinia: Precambrian Research, v. 113, p. 135–154, doi: 10.1016/S0301-9268(01)00207-8.

Li, X. H., Li, Z. X., Ge, W., Zhou, H., Li, W., Liu, Y., and Wingate, M. T. D., 2003a, Neoproterozoic granitoids in South China: crustal melting above a mantle plume at ca. 825 Ma?: Precambrian Research, v. 122, p. 45–83, doi: 10.1016/S0301-9268(02)00207-3.

Li, X. H., Li, Z. X., Zhou, H. W., Liu, Y., Liang, X. R., and Li, W. X., 2003b, SHRIMP U-Pb zircon age, geochemistry and Nd isotope of the Guandaoshan pluton in SW Sichuan: Petrogenesis and tectonic significance: Science in China (Series D), v. 46, Supplement, p. 73–83, doi: 10.1360/03dz9029.

Li, X. H., Liu, D. Y., Sun, M., Li, W. X., Liang, X. R., and Liu, Y., 2004, Precise Sm-Nd and U-Pb isotopic dating of the super-giant Shizhuyuan polymetallic deposit and its host granite: Southeast China: Geological Magazine, v. 141, p. 225–231, doi: 10.1017/S0016756803008823.

Li, X. H., Qi, C. S., Liu, Y., Liang, X. R., Tu, X. L., Xie, L. W., and Yang, Y. H., 2005, Petrogenesis of the Neoproterozoic bimodal volcanic rocks along the western margin of the Yangtze Block: New constraints from Hf isotopes and Fe/Mn ratios: Chinese Science Bulletin, v. 50, p. 2481–2486, doi: 10.1360/982005-287.

Li, X. H., Li, Z. X., Sinclair, J. A., Li, W. X., and Carter, G., 2006, Revisiting the "Yanbian Terrane": Implications for Neoproterozoic tectonic evolution of the western Yangtze Block, South China: Precambrian Research, v. 151, p. 14–30, doi: 10.1016/j.precamres.2006.07.009.

——— 2007, Reply to the comment by Zhou et al. on: "Revisiting the 'Yanbian Terrane': Implications for Neoproterozoic tectonic evolution of the western Yangtze Block, South China"—[Precambrian Res. 151 (2006) 14-30]—[Precambrian Res. 154 (2007) 153-157]: Precambrian Research, v. 155(3-4), p. 318–323, doi: 10.1016/j.precamres.2006.11.012.

Li, X. H., Li, W. X., Li, Z. X., and Liu, Y., 2008, 850–790 Ma bimodal volcanic and intrusive rocks in northern Zhejiang, South China: A major episode of continental rift magmatism during the breakup of Rodinia: Lithos, v. 102, p. 341–357, doi: 10.1016/j.lithos.2007.04.007.

Li, X. H., Li, W. X., Li, Z. X., Lo, C. H., Wang, J., Ye, M. F., and Yang, Y. H., 2009a, Amalgamation between the Yangtze and Cathaysia Blocks in South China: Constraints from SHRIMP U-Pb zircon ages, geochemistry and Nd-Hf isotopes of the Shuangxiwu volcanic rocks: Precambrian Research, v. 174, p. 117–128, doi: 10.1016/j.precamres.2009.07.004, doi: 10.1016/j.precamres.2009.07.004.

Li, X. H., Liu, Y., Li, Q. L., Guo, C. H., and Chamberlain, K. R., 2009b. Precise determination of Phanerozoic zircon Pb/Pb age by multi-collector SIMS without external standardization: Geochemistry Geophysics Geosystems, v. 10, Q04010, doi: 10.1029/2009GC002400.

Li, X. H., Li, W. X., Li, Q. L., Wang, X. C., Liu, Y., and Yang, Y. H., 2010, Petrogenesis and tectonic significance of the ~850 Ma Gangbian alkaline complex in South China: Evidence from *in-situ* zircon U-Pb dating, Hf-O isotopes and whole-rock geochemistry: Lithos, v. 114, p. 1–15, doi: 10.1016/j.lithos.2009.07.011.

Li, Z. X., and Zhong, S., 2009, Supercontinent-superplume coupling, true polar wander and plume mobility: Plate dominance in whole-mantle tectonics: Physics of the Earth and Planetary Interiors, v. 176, p. 143–156 doi: 10.1016/j.pepi.2009.05.004.

Li, Z. X., Li, X. H., Kinny, P. D., and Wang, J., 1999, The breakup of Rodinia: did it start with a mantle plume beneath South China?: Earth and Planetary Science Letters, v. 173, p. 171–181, doi: 10.1016/S0012-821X(99)00240-X.

Li, Z. X., Li, X. H., Zhou, H. W., and Kinny, P. D., 2002, Grenvillian continental collision in south China: New SHRIMP U-Pb zircon results and implications for the configuration of Rodinia: Geology, v. 30, p. 163–166, doi: 10.1130/0091-7613(2002)030<0163:GCCISC>2.0.CO;2.

Li, Z. X., Li, X. H., Kinny, P. D., Wang, J., Zhang, S., and Zhou, H., 2003, Geochronogly of Neoproterozoic syn-rift magmatism in the Yangtze Craton South China and correlations with other continents: evidence for a mantle superplume that broke up Rodinia: Precambrian Research, v. 122, p. 85–109, doi: 10.1016/S0301-9268(02)00208-5.

Li, Z. X., Evans, D. A. D., and Zhang, S., 2004, A 90° Spin on Rodinia: Possible causal links between the Neoproterozoic supercontinent, superplume, true polar wander and low-latitude glaciation: Earth and Planetary Science Letters, v. 220, p. 409–421, doi: 10.1016/S0012-821X(04)00064-0.

Li, Z. X., Wartho, J. A., Occhipinti, S., Zhang, C. L., Li, X. H., Wang, J., and Bao, C. M., 2007, Early history of the eastern Sibao Orogen (South China) during the assembly of Rodinia: New mica $^{40}Ar/^{39}Ar$ dating and SHRIMP U-Pb detrital zircon provenance constraints: Precambrian Research, v. 159, p. 79–94, doi: 10.1016/j.precamres.2007.05.003.

Li, Z. X., Bogdanova, S. V., Collins, A. S., Davidson, A., De Waele, B., Ernst, R. E., Fitzsimons, I. C. W., Fuck, R. A., Gladkochub, D. P., Jacobs, J., Karlstrom, K. E., Lu, S., Natapov, L. M., Pease, V., Pisarevsky, S. A., Thrane, K., and Vernikovsky, V., 2008, Assembly, configuration, and breakup history of Rodinia: A synthesis: Precambrian Research, v. 160, p. 179–210, doi: 10.1016/j.precamres.2007.04.021.

Li, Z. X., Li, X. H., Wartho, J. A., Clark, C., Li, W. X., Zhang, C. L., and Bao, C., 2010, Magmatic and metamorphic events during the Early Paleozoic Wuyi-Yunkai Orogeny, southeastern South China: New age constraints and P-T conditions: The Geological Society of America Bulletin, v. 122, p. 772–793, doi: 10.1130/B30021.1.

Lin, G. C., Li, X. H., and Li, W. X., 2007, SHRIMP U-Pb zircon age, geochemistry and Nd-Hf isotope of Neoproterozoic mafic dyke swarms in western Sichuan: Petrogenesis and tectonic significance: Science in China (series D), v. 50, p. 1–16, doi: 10.1007/s11430-007-2018-0.

Ludwig, K. R., 2001, Users manual for Isoplot/Ex rev. 2.49: Berkeley Geochronology Center Special Publication, No. 1a, 56 p.

McCulloch, M. T., and Gamble, J. A., 1991, Geochemical and geodynamical constraints on subduction zone magmatism: Earth and Planetary Sciences Letters, v. 102, p. 358–374, doi: 10.1016/0012-821X(91)90029-H.

Millar, I. L., 1999, Neoproterozoic extensional basic magmatism associated with the West Highland granite gneiss in the Moine Supergroup of NW Scotland: Journal of the Geological Society, London, v. 156, p. 1153–1162, doi: 10.1144/gsjgs.156.6.1153.

Miyashiro, A., 1974, Volcanic rock series in island arc and active continental margins: American Journal of Science, v. 274, p. 321–355, doi: 10.2475/ajs.274.4.321.

Moores, E. M., 1991, Southwest U.S.-East Antarctic (SWEAT) connection: A hypothesis: Geology, v. 19, p. 425–428, doi: 10.1130/0091-7613(1991)019<0425:SUSEAS>2.3.CO;2.

Morrison, M. A., 1978, The use of "immobile" trace elements to distinguish the palaeotectonic affinities of metabasalts: Applications to the Paleocene basalts of Mull and Skye, northwest Scotland: Earth and Planetary Science Letters, v. 39, p. 407–416, doi: 10.1016/0012-821X(78)90029-8.

Mysen, B. O., and Boettcher, A. L., 1975, Melting of hydrous mantle: I. Phase relations of natural peridotite at high pressures and temperatures with controlled activities of water, carbon dioxide and hydrogen: Journal of Petrology, v. 16, p. 520–548, doi: 10.1093/petrology/16.3.520.

Nasdala, L., Hofmeister, W., Norberg, N., Mattinson, J. M., Corfu, F., Dörr, W., Kamo, S. L., Kennedy, A. K., Kronz, A., Reiners, P. W., Frei, D., Kosler, J., Wan, Y., Götze J., Häger, T., Kröner, A., and Valley, J. W., 2008, Zircon M257—a homogeneous natural reference material for the ion microprobe U-Pb analysis of zircon: Geostandards and Geoanalytical Research, v. 32, p. 247–265, doi: 10.1111/j.1751-908X.2008.00914.x.

Nesbitt, H. W., and Young, G. M., 1982, Early Proterozoic climates and plate motions inferred from major element chemistry of lutites: Nature, v. 299, p. 715–717, doi: 10.1038/299715a0.

——— 1989, Formation and diagenesis of weathering profiles: The Journal of Geology, v. 97, p. 129–147, doi: 10.1086/629290.

Paulsson, O., and Andreasson, P. G., 2002, Attempted break-up of Rodinia at 850 Ma: geochronological evidence from the Seve-Kalak Superterrane, Scandinavian Caledonides: Journal of the Geological Society, London, v. 159, p. 751–761, doi: 10.1144/0016-764901-156.

Pearce, J. A., and Cann, J. R., 1973, Tectonic setting of basic volcanic rocks determined using trace element analysis: Earth and Planetary Science Letters, v. 19, p. 290–300, doi: 10.1016/0012-821X(73)90129-5.

Peccerillo, A., Barberio, M. R., Yirgu, G., Ayalew, D., Barbieri, M., and Wu, T. W., 2003, Relationships between mafic and peralkaline silicic magmatism in continental rift settings: a petrological, geochemical and isotopic study of the Gedemsa Volcano, Central Ethiopian Rift: Journal of Petrology, v. 44, p. 2003–2032, doi: 10.1093/petrology/egg068.

Pin, C., and Paquette, J. L., 1997, A mantle-derived bimodal suite in the Hercynian Belt: Nd isotope and trace element evidence for a subduction-related rift origin of the Late Devonian Brévenne metavolcanics, Massif Central (France): Contributions to Mineralogy and Petrology, v. 129, p. 222–238, doi: 10.1007/s004100050334.

Rollinson, H. R., 1993, Using Geochemical Data: Evaluation, Presentation, Interpretation: London, Longman Publishing Group, p. 1–352.

Romer, R. L., Forster, H. J., and Breitkreuz, C., 2001, Intracontinental extensional magmatism with a subduction fingerprint: the late Carboniferous Halle Volcanic Complex (Germany): Contributions to Mineralogy and Petrology, v. 141, p. 201–221, doi: 10.1007/s004100000231.

Shervais, J. W., 1982, Ti-V plots and the petrogenesis of modern and ophiolitic lavas: Earth and Planetary Science Letters, v. 59, p. 101–118, doi: 10.1016/0012-821X(82)90120-0.

Soper, N. J., Harris, A. L., and Strachan, R. A., 1998, Tectonostratigraphy of the Moine Supergroup: a synthesis: Journal of the Geological Society, London, v. 155, p. 13–24, doi: 10.1144/gsjgs.155.1.0013.

Stacey, J. S., and Kramers, J. D., 1975, Approximation of terrestrial lead isotope evolution by a two-stage model: Earth and Planetary Science Letters, v. 26, 207–221, doi: 10.1016/0012-821X(75)90088-6.

Sun, S. S., and McDonough, W. F., 1989, Chemical and isotopic systematics of oceanic basalt: Implications for mantle composition and processes, *in* Sanders, A. D., and Norry, M. J. editors, Magmatism in the Ocean Basins: Geological Society, London, Special Publications, v. 42, 528–548, doi: 10.1144/GSL.SP.1989.042.01.19.

Sun, W. H., and Zhou, M. F., 2008, The 860-Ma, Cordilleran-type Guandaoshan Dioritic Pluton in the Yangtze Block, SW China: Implications for the Origin of Neoproterozoic Magmatism: Journal of Geology, v. 116, p. 238–253, doi: 10.1086/587881.

Suneson, N. H., and Lucchita, I., 1983, Origin of bimodal volcanism, southern Basin and Range province, west-central Arizona: Geological Society of America Bulletin, v. 94, p. 1005–1019, doi: 10.1130/0016-7606(1983)94<1005:OOBVSB>2.0.CO;2.

Tanaka, T., Togashi, S., Kamioka, H., Amakawa, H., Kagami, H., Hamamoto, T., Yuhara, M., Orihashi, Y., Yoneda, S., Shimizu, H., Kunimaru, T., Takahashi, K., Yanagi, T., Nakano, T., Fujimaki, H., Shinjo, R., Asahara, Y., Tanimizu, M., and Dragusanu, C., 2000, JNdi-1: a neodymium isotopic reference in consistency with LaJolla neodymium: Chemical Geology, v. 168, p. 279–281, doi: 10.1016/S0009-2541(00)00198-4.

Tatsumi, Y., and Eggins, S. M., 1995, Subduction Zone Magmatism: Cambridge, Blackwell Science, p. 211.

Teagle, D. A. H., and Alt, J. C., 2004, Hydrothermal alteration of Basalts beneath the Bent Hill Massive Sulfide Deposit, Middle Valley, Juan De Fuca Ridge: Economic Geology, v. 99, p. 561–584, doi: 10.2113/99.3.561.

Vermeesch, P., 2006, Tectonic discrimination diagrams revisited: Geochemistry Geophysics Geosystems, v. 7, Q06017. doi: 10.1029/2005GC001092, doi: 10.1029/2005GC001092.

Wang, J., and Li, Z. X., 2003, History of Neoproterozoic rift basins in South China: implications for Rodinia break-up: Precambrian Research, v. 122, p. 141–158, doi: 10.1016/S0301-9268(02)00209-7.

Wang, X. C., Li, X. H., Li, W. X., and Li, Z. X., 2007, Ca. 825 Ma komatiitic basalts in South China: First evidence for >1500°C mantle melts by a Rodinian mantle plume: Geology, v. 35, p. 1103–1106, doi: 10.1130/G23878A.1.

Wang, X. C., Li, X. H., Li, W. X., Li, Z. X., Liu, Y., Yang, Y. H., Liang, X. R., and Tu, X. L., 2008, The Bikou basalts in northwestern Yangtze Block, South China: Remnants of 820–810 Ma continental flood basalts?: Geological Society of America Bulletin, v. 120, p. 1478–1492, doi: 10.1130/B26310.1, doi: 10.1130/B26310.1.

Wang, X. C., Li, X. H., Li, W. X., and Li, Z. X., 2009, Variable involvements of mantle plumes in the genesis of mid-Neoproterozoic basaltic rocks in South China: A review: Gondwana Research, v. 15, p. 381–395, doi: 10.1016/j.gr.2008.08.003.

Wang, X. L., Zhou, J. C., Qiu, J. S., Zhang, W. L., Liu, X. M., and Zhang, G. L., 2006, LA-ICP-MS U-Pb zircon geochronology of the Neoproterozoic igneous rocks from Northern Guangxi, South China: Implications for tectonic evolution: Precambrian Research, v. 145, p. 111–130, doi: 10.1016/j.precamres.2005.11.014.

Wang, X. L., Zhou, J. C., Griffin, W. L., Wang, R. C., Qiu, J. S., O'Reilly, S. Y., Xu, X., Liu, X. M., and Zhang, G. L., 2007, Detrital zircon geochronology of Precambrian basement sequences in the Jiangnan orogen: Dating the assembly of the Yangtze and Cathaysia Blocks: Precambrian Research, v. 159, p. 117–131, doi: 10.1016/j.precamres.2007.06.005.

Wang, X. L., Zhao, G. C., Zhou, J. C., Liu, Y. S., and Hu, J., 2008, Geochronology and Hf isotopes of zircon from volcanic rocks of the Shuangqiaoshan Group, South China: Implications for the Neoproterozoic tectonic evolution of the eastern Jiangnan orogen: Gondwana Research, v. 14, p. 355–367, doi: 10.1016/j.gr.2008.03.001.

Wilson, M., 1989, Igneous Petrogenesis: London, Unwin Hyman, p. 466.

Winchester, J. A., and Floyd, P. A., 1976, Geochemical magma type discrimination: application to altered and metamorphosed basic igneous rocks: Earth and Planetary Science Letters, v. 28, p. 459–469, doi: 10.1016/0012-821X(76)90207-7.

Wu, R. X., Zheng, Y. F., Wu, Y. B., Zhao, Z. F., Zhang, S. B., Liu, X. M., and Wu, F. Y., 2006, Reworking of juvenile crust: Element and isotope evidence from Neoproterozoic granodiorite in South China: Precambrian Research, v. 146, p. 179–212, doi: 10.1016/j.precamres.2006.01.012.

Ye, M. F., Li, X. H., Li, W. X., Liu, Y., and Li, Z. X., 2007, SHRIMP zircon U-Pb geochronological and whole-rock geochemical evidence for an early Neoproterozoic Sibaoan magmatic arc along the southeastern margin of the Yangtze Block: Gondwana Research, v. 12, p. 144–156, doi: 10.1016/j.gr.2006.09.001.

Young, G. M., 2009, Geochemical investigation of an unusual alteration profile developed at the base of a Carboniferous lava flow, Isle of Bute, Scotland: Earth and Environmental Science Transactions of the Royal Society of Edinburgh, v. 99, p. 49–59, doi: 10.1017/S1755691009007038.

Zhong, S., Zhang, N., Li, Z. X., and Roberts, J. H., 2007, Supercontinent cycles, true polar wander, and very long-wavelength mantle convection: Earth and Planetary Science Letters, v. 261, p. 551–564, doi: 10.1016/j.epsl.2007.07.049.

Zhou, J. C., Wang, X. L., and Qiu, J. S., 2009, Geochronology of Neoproterozoic mafic rocks and sandstones from northeastern Guizhou, South China: Coeval arc magmatism and sedimentation: Precambrian Research, v. 170, p. 27–42, doi: 10.1016/j.precamres.2008.11.002.